




Review

Metal–Organic Frameworks as Versatile Platforms for Organometallic Chemistry

Fan Chen ¹, Hannah F. Drake ¹ , Liang Feng ¹, Joshua A. Powell ¹ , Kun-Yu Wang ¹, Tian-Hao Yan ¹ and Hong-Cai Zhou ^{1,2,*} 

¹ Department of Chemistry, Texas A&M University, College Station, TX 77843-3255, USA; fanchen2018@tamu.edu (F.C.); hfd100@tamu.edu (H.F.D.); fengliang@tamu.edu (L.F.); jpowell7@tamu.edu (J.A.P.); wangkuny@tamu.edu (K.-Y.W.); thyan426@tamu.edu (T.-H.Y.)
² Department of Materials Science and Engineering, Texas A&M University, College Station, TX 77843-3003, USA
 * Correspondence: zhou@chem.tamu.edu

Abstract: Metal–organic frameworks (MOFs) are emerging porous materials with highly tunable structures developed in the 1990s, while organometallic chemistry is of fundamental importance for catalytic transformation in the academic and industrial world for many decades. Through the years, organometallic chemistry has been incorporated into functional MOF construction for diverse applications. Here, we will focus on how organometallic chemistry is applied in MOF design and modifications from linker-centric and metal-cluster-centric perspectives, respectively. Through structural design, MOFs can function as a tailorable platform for traditional organometallic transformations, including reaction of alkenes, cross-coupling reactions, and C–H activations. Besides, an overview will be made on other application categories of organometallic MOFs, such as gas adsorption, magnetism, quantum computing, and therapeutics.

Keywords: metal–organic framework; organometallic; coordination bonds; supramolecular chemistry; catalysis



Citation: Chen, F.; Drake, H.F.; Feng, L.; Powell, J.A.; Wang, K.-Y.; Yan, T.-H.; Zhou, H.-C. Metal–Organic Frameworks as Versatile Platforms for Organometallic Chemistry. *Inorganics* **2021**, *9*, 27. <https://doi.org/10.3390/inorganics9040027>

Academic Editor: Andrea Rossin

Received: 2 March 2021

Accepted: 1 April 2021

Published: 9 April 2021

Publisher's Note: MDPI stays neutral with regard to jurisdictional claims in published maps and institutional affiliations.



Copyright: © 2021 by the authors. Licensee MDPI, Basel, Switzerland. This article is an open access article distributed under the terms and conditions of the Creative Commons Attribution (CC BY) license (<https://creativecommons.org/licenses/by/4.0/>).

1. Introduction

Catalytic transformations to design new and tailored commodity items have been of interest for many decades, both in the private, industrial, and academic world. This success is owed in part to the catalytic transformations of organometallic complexes, their functionalizable environments, and their active centers. Many important industrial processes that we rely upon in our modern lifestyle depend on the basic chemical transformations using organometallic chemical processes. In particular, the chemical transformations used to generate ammonia, synthesis gas, epoxyethane, sulfuric acid, nitric acid, and many polymer-based plastics involve an organometallic catalyst (iron, nickel, silver on alumina, vanadium, platinum and rhodium, and titanium respectively) [1]. It is estimated that 300 million tons of polymer-based plastics alone are produced globally each year at least in part from catalytic synthesis processes [2–4]. This area of research has long been a key feature in the modernization and globalization of our world as many of the everyday commodities we utilize are made through organometallic chemical processes. Thus, there are also many new approaches to design better and more effective ways of producing these commodities by further refining the organometallic catalytic processes that are utilized most heavily today. Among these approaches, Metal–organic frameworks (MOFs) have taken a central role in the improvement of organometallic catalytic research.

Within our context, MOFs, also known as porous coordination networks (PCNs), are a type of highly crystalline, well ordered coordination network compounds derived from both metal and organic components. MOFs originated in the late 1990s with seminal works published from Yaghi and Kitagawa and is thus still a very recent advance towards catalytic

chemical systems [5,6]. Despite their relative infancy as a field, these materials are rapidly becoming well known for their versatility due to their diverse tunability of the linkers, pore voids, and metal nodes that make up the three key features of these structures [7–10]. Although MOFs are not considered to be traditional organometallic compounds in the most restrictive definition of organometallic chemistry, as many of them do not contain M–C bonds, the unique tunability and ability to design tailored chemical reactions allows MOFs to undergo many of the same chemical processes used in M–C type organometallic chemistry. Within MOF structures, most of the organic linker coordination bonds that hold the structures together are comprised of N, O, or S donor atom to metal cluster bonds [11]. Ultimately, many MOFs discussed in this review do perform catalytic organometallic M–C type chemistry as the scaffold material even though the scaffold itself is a coordination type complex [12–16].

The three main components of MOFs are their linkers, void spaces, and metal clusters. All three of these features can be tuned specifically towards desired transformations. For the purposes of this review, we will emphasize two main features of interest: the functionalization of organic linkers towards catalytic chemistry and the transformation of metal cluster centers towards these processes. We will expand upon the utilization of MOFs for traditional organometallic chemical applications, demonstrate the current directions of non-traditional utilization of MOFs in organometallic catalytic process, and give an outlook on the future directions of this field (Figure 1).

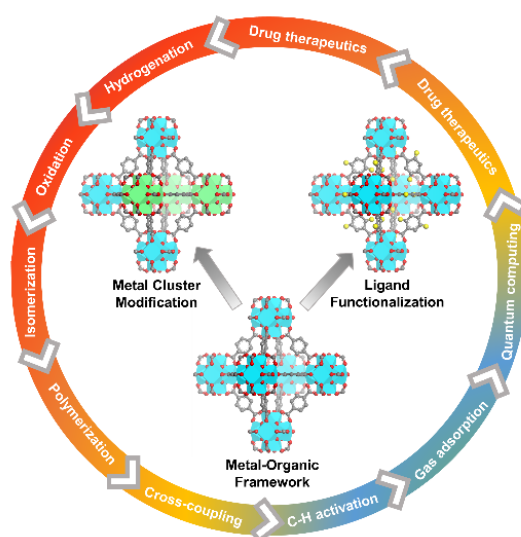


Figure 1. Summarizing figure of organometallic chemistry in metal–organic frameworks. Blue = Zr atoms. Green = Hf atoms. Red = O atoms. Grey = C atoms. Yellow = F atoms.

2. Linker-Based Functional Organometallic MOFs

MOFs are a class of crystalline porous material that have attracted considerable attention over the past few decades [17]. Due to their permanent porosity, large surface area, structural and functional diversity, and tunability, MOFs have been utilized in a diverse array of applications. Some of these applications include: gas sorption and separation, chemical sensing, proton conduction, and drug delivery [18–23]. Of particular interest, MOFs are considered to be promising candidates as heterogeneous organometallic catalysts [19–24]. For catalytic applications, MOFs offer two approaches: cluster mediated catalysis and linker mediated catalysis. The organic linker building block plays an important part in the reasonable design of MOF-based catalysts [25]. In this section, linker-based organometallic catalysis will be discussed. Additionally, the relationship between MOF structure and application will also be discussed.

2.1. Porphyrin-Based Linkers

Porphyrin chemistry has been of significant biological interest. It is no wonder that porphyrin-based ligands would be of significant interest for MOF chemistry, particularly in light-harvesting, sensing, and catalysis [26]. As a result, porphyrin ligand-based MOFs have been substantially explored. Building porphyrins into MOF scaffolds eliminates the dimerization pathways and mitigates the solubility and chemical stability issues often associated with porphyrin chemistry. In return, porphyrins add additional functionality to the MOF scaffold, particularly in photo-sensing catalysis [27]. As a result, the introduction of porphyrins into MOFs as linkers has allowed for scientists to take advantage of both systems.

One example of a porphyrin-based MOFs came from the Zhou group, PCN-224. This MOF was assembled from 6-connected Zr_6 secondary building units (SBUs) and metalloporphyrin ligands (Fe-TCPP (TCPP = tetrakis(4-carboxyphenyl)-porphyrin)) (Figure 2), into a 3D nanochanneled, highly stable framework. PCN-224 has been utilized as a highly active, recoverable heterogeneous catalyst in CO_2 /propylene oxide coupling reactions [28]. PCN-224(Ni) was tested to be extra stable for the remained property after 24 h immersion in over a wide range of pH in aqueous solution, from 1 to 11. Expanding upon this initial study, a series of PCN-224 analogues with ethyl, bromo, chloro, and fluoro to the β -position of porphyrin ligands was synthesized. This series was shown to be able to tune the chemical environment of the catalytic center for desired reactions by changing the electronic properties in the ligand scaffold. In this work it was also demonstrated that a substitution within the TCPP linker was able to increase the activity and selectivity of the catalytic iron sites in the 3-methylpentane oxidation catalysis [29].

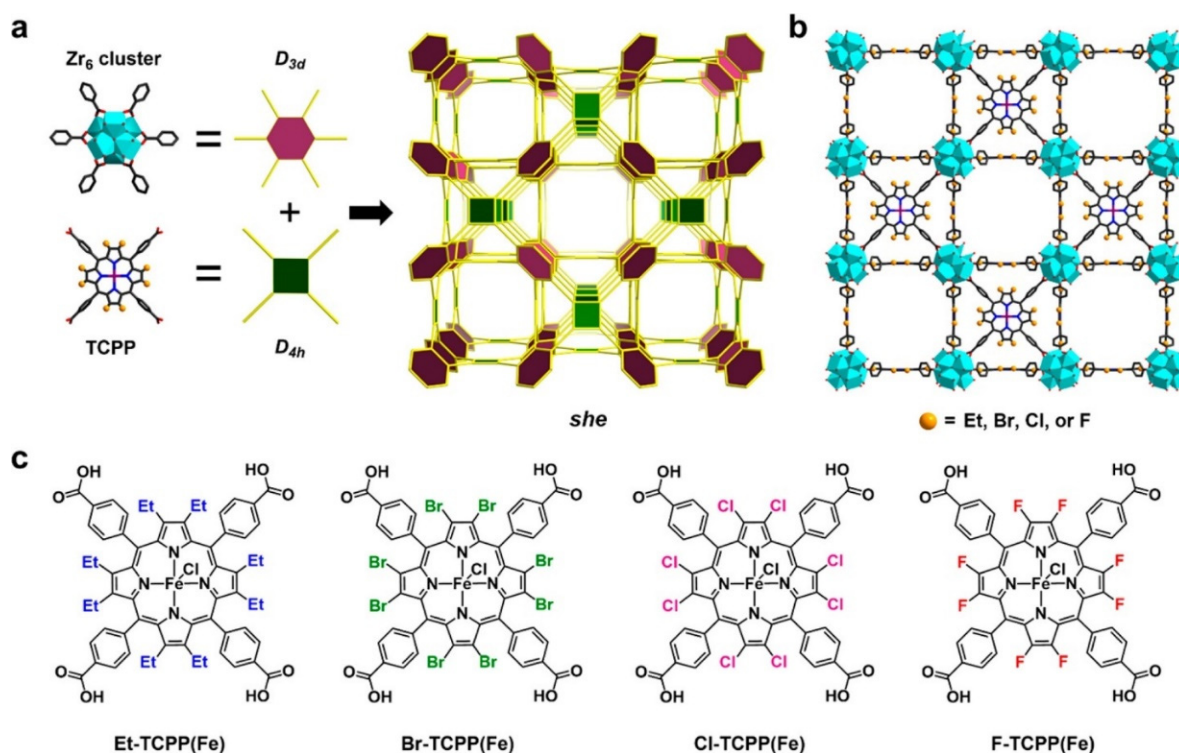


Figure 2. (a) Assembly of D_{3d} and D_{4h} nodes into (4,6)-connected *she* topological network. The Zr_6 cluster and TCPP(Fe) ligand can be viewed as 6- and 4-connected nodes, respectively. (b) View down the tetragonal channels of R-PCN-224(Fe) (black, carbon; purple, iron; blue, nitrogen; hydrogen and chloride, omitted). The yellow spheres represent Et, Br, Cl, or F. (c) Chemical structures of Et-TCPP(Fe), Br-TCPP(Fe), Cl-TCPP(Fe), and F-TCPP(Fe) linkers. Adapted with permission from [29]; Published by American Chemical Society, 2017.

Porphyrinic linkers can also be utilized as photosensitive building blocks in MOFs. Post-synthetic metalation of metal-free porphyrins is a common way of adjusting the catalytic property of porphyrins-based MOF. One particular example from the Rosseinsky group reported an aluminum-based porous porphyrin MOF that could perform water splitting under visible light irradiation. Within the rigid host structure of this MOF, the metal-free porphyrins could be metalated with Zn^{2+} , allowing for the catalytic generation of hydrogen and oxygen from water [30]. Another example of a post-synthetic metalation of porphyrin for tuned catalytic reactions is PCN-223, showing high stability in aqueous solutions with a wide range of pH due to its extremely high connectivity. This metal-free porphyrin Zr-MOF was metalated with Fe^{3+} , making it an excellent recyclable catalyst for hetero-Diels–Alder reactions [31].

In another work, a robust metalloporphyrinic MOF with perfluorophenylene functional groups, PCN-624, was synthesized utilizing rational structure design techniques. PCN-624 was constructed from 12-connected $[\text{Ni}_8(\text{OH})_4(\text{H}_2\text{O})_2\text{Pz}_{12}]$ (Pz = pyrazolide) nodes and fluorinated 5,10,15,20-tetrakis-(2,3,5,6-tetrafluoro-4-(1H-pyrazol-4-yl)phenyl)-porphyrin (TTFPPP) ligands. Pendant perfluorophenylene groups were fabricated onto the pore surface of PCN-624, resulting in the cyclable, selective synthesis of fullerene-anthracene bis-adducts. This example also demonstrates that MOFs can be utilized as a competitive platform for catalytic applications [32].

2.2. Polypyridyl-Based Linkers

In recent years, harvesting solar power through light harvesting materials has received interest in the scientific community in the application of renewable energy sources. The utilization of polypyridyl organometallic complexes in light harvesting devices is fairly well developed. As a result, MOFs designed for light harvesting have begun to incorporate polypyridyl moieties into their frameworks. This approach has attracted interest for applications in catalytic water oxidation, CO_2 reduction, photocatalytic hydrogen evolution, and the photocatalysis of organic reactions [25].

One of the pioneer research groups for doping polypyridyl organometallic complexes into MOFs, the Lin group, demonstrated the usability of this system for solar energy harvesting. In 2011, this group incorporated Ir, Re, and Ru polypyridyl complexes into the UiO-67 (UiO = University of Oslo) topology, leading to a series of highly active heterogeneous catalysts for visible light-driven organic molecule transformations [33]. Later, the same group merged a Ir^{III} photoredox catalyst and a Ni^{II} cross-coupling catalyst into the same MOF scaffold to efficiently catalyze C-S bond formation between different aryl iodides and thiols [34].

Among organic transformations through organometallic catalysis, CO_2 reduction is one that is of particular interest, since CO_2 and CH_4 are widely known to be of use in chemical energy conversions. One approach to accomplish CO_2 reduction is through molecular iridium catalysts immobilized within a MOF. In one such study, Ir–UiO MOFs, mbpyOH– IrCl_3 –UiO and mbpy IrCl_3 –UiO (bpy = 2,2'-bipyridine), were synthesized and placed in a condensation chamber, facilitating CO_2 reduction [12]. In another study, a metal-organic layer (MOL), a freestanding monolayer of a 2D MOF, was utilized as a novel platform for CO_2 hydrogenation. As a result of modifications made to the Hf_{12} SBUs and the $[\text{Ru}(\text{bpy})_3]^{2+}$ based linkers in the study, a new kind of MOL was prepared that showed efficient catalytic performance for the reduction of CO_2 [35]. The structural stability of the MOLs was approved by the repeatable PXRD (powder X-ray diffraction) patterns after 24 h of CO_2 reduction.

An azide-functionalized UiO-66 was employed as a platform for the immobilization of a series of bidentate ligands on a MOF surface via an azide-alkyne “click” reaction. These immobilized ligands formed a highly effective mixed-ligand nickel catalyst. The product generated was demonstrated to be an effective heterogeneous organometallic catalyst for the Suzuki–Miyaura coupling reaction under mild conditions. The system was also shown

to be recyclable with little to no change to the performance or properties of the original material [36].

An example of a metalloporphyrin MOF that is active towards C–H activation is PCN-602, which was reported by the Zhou group. This MOF is a base-resistant porphyrin-based system built from $[\text{Ni}_8(\text{OH})_4(\text{H}_2\text{O})_2\text{Pz}_{12}]$ (Pz = pyrazolate) clusters and 5,10,15,20-tetrakis(4-(pyrazolate-4-yl)-phenyl)porphyrin linkers [37]. The derived PCN-602(Mn) with Mn^{3+} -porphyrin centers was used to catalyze C–H bond chlorination and bromination reactions for cyclohexane and cyclopentane reactions, demonstrating good performance. The metalated porphyrin species as a catalyst was able to yield a 95% conversion rates under room temperature conditions after 2 h. These results indicated that this particular MOF was a highly effective catalyst for C–H halogenation of hydrocarbons under basic conditions. Moreover, PCN-602 exhibited great stability in aqueous solutions of OH^- , F^- , CO_3^{2-} , and PO_4^{3-} .

2.3. Pyridyl-Based Linkers

One of the earliest examples of a pyridyl-based MOFs comes from the Humphrey group who prepared the first organoarsine MOF, ACM-1, using a new pyridyl-functionalized triarylsarsine ligand coordinated to Ni^{II} nodes. Under facile conditions, postsynthetic metalation of the ACM-1 structure was accomplished through the installation of dimeric Au_2Cl_2 complexes via the formation of As–Au bonds. Due to the rigidity of the MOF, the Au^{I} dimers displayed particularly short aurophilic bonds (2.76 Å) [38].

With growing focus on pyridyl-based MOFs, postsynthetic modifications are now fairly common. An example of this was with a Zr-MOF scaffold that was modified to obtain a bimetallic MOF with $\text{MX}_2(\text{INA})_4$ moieties (INA = isonicotinate; $\text{M} = \text{Co}^{2+}$ or Fe^{2+} ; $\text{X} = \text{OH}^-$, Cl^- , Br^- , I^- , NCS^- , or NCSe^-). The step-by-step modification process not only changed the composition, symmetry, and unit cell of the MOF by introducing $\text{MX}_2(\text{py})_4$ (py = pyridine), but the exchange also endowed interesting magnetic and electronic properties to the diamagnetic framework [39].

MOFs serve as designable platforms to construct complex coordination architectures for desirable applications. A method to place trans-coordinate metal centers with exposed equatorial positions in a MOF matrix has been reported. PCN-160, a Zr-based MOF, was initially synthesized and subsequently underwent postsynthetic modification in the form of ligand elimination and installation of pyridinecarboxylate ligands (Figure 3). The proximity between a pair of neighboring pyridyl groups within the ligand was suitable for the formation of trans-metal-binding sites that were capable of accepting multiple diatomic metal cations. Some metals tested in this body of work included: Ni^{2+} , Cu^{2+} , and Pd^{2+} . This particular trans-coordinated metal site in the MOF was utilized for the catalytic dimerization of ethylene. This catalyst in particular had high activity due to the exposed equatorial positions of the open metal sites [40].

2.4. Pincer-Based Linkers

Ligands that chelate a metal using three coplanar chelators are referred to as pincer ligands. In organometallic chemistry, pincer complexes have been extensively shown to be remarkable catalysts for a variety of applications [41]. It is no surprise then that pincer-based ligands have begun to be incorporated into MOFs in recent years. One such example is for a Zr-based MOF with modified Pd aryl diphosphinite (POCOP) pincer linkers. This particular system was shown to be remarkably active and recyclable as a catalyst for the transfer hydrogenation of benzaldehydes, together with the exceptional chemical stability even under strong acid (1 M HNO_3) and base (0.1 M NaOH) for weeks [15]. Typically pincer-based ligands require postsynthetic metalation of the chelation site otherwise the as synthesized MOF fails to form. There are very few reports of pincer-based MOFs that do not require this post synthetic step. One such MOF, a 3D MOF Co^{II} MOF was synthesized through first cyclometallation of the pincer ligand with $\text{Pd}^{\text{II}}\text{Cl}$ and subsequent use of the

metalloligand as a starting material in a one pot solvothermal reaction. The Pd–Cl groups in the chelation site were highly catalytically active for CO₂ insertion at 1atm and 298 K [42].

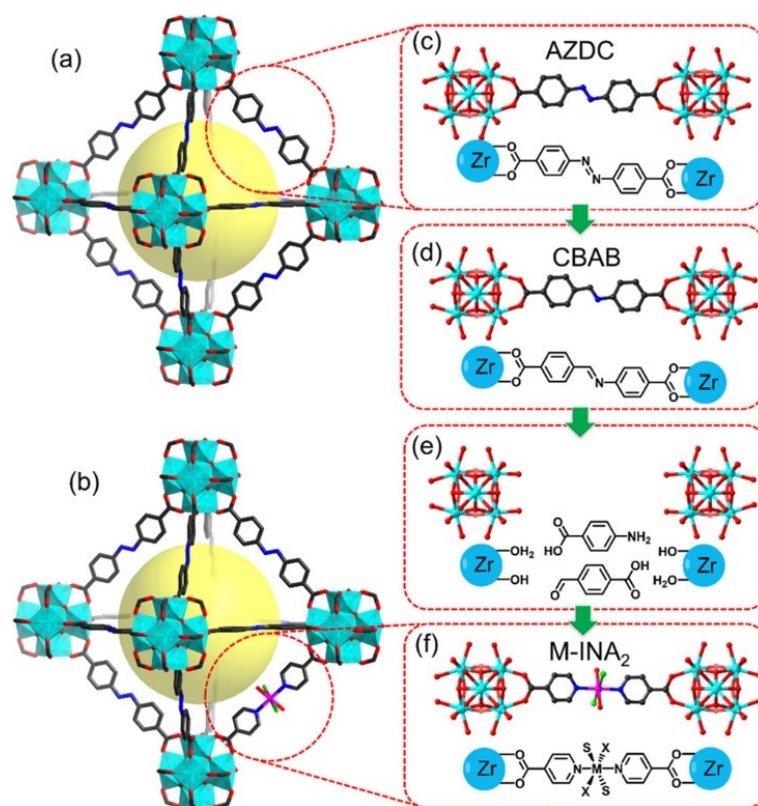


Figure 3. Structure of PCN-160 (a) and PCN-160-R%M with *trans*-chelating ligands (b). Transformation of ligand fragment in PCN-160 (c) by CBAB exchange (d), linker labialization (e), and installation of M-INA₂ (INA = isonicotinate) (f). These figures are based on respective single-crystal structures after removal of the disordered fragments. Cyan = Zr. Red = O. Grey = C. Blue = N. Adapted with permission from [40]; Published by American Chemical Society, 2018.

2.5. Other Linkers in MOFs

In addition to the porphyrins, polypyridyl, and pincer ligands discussed in this section, there have been other organometallic catalytic linkers that have been incorporated into MOFs. For example, N-heterocyclic carbene-based linkers (NHC) have been incorporated into MOF frameworks for catalytic applications. For these linkers, tuning the imidazole sidechains with different functional groups offers a dynamic array of possible catalytic activity. One example of an NHC-based MOF was published by the Zou group and contained an Iridium NHC metallolinker in a Zr-MOF. Through both direct synthesis and postsynthetic exchange, the MOF was able to be synthesized and adapted for allylic alcohol isomerization. This particular MOF demonstrated good catalytic activity and recyclability [43].

3. Cluster-Based Functional Organometallic MOFs

Metal clusters are widely known to be Lewis acidic sites within MOF structures. However, recent work has also explored the use of metal clusters within MOFs as organometallic catalysts and as a platform for the support of single-site organometallic catalysts. Single-site catalysts are preferred over metal oxide or metal nanoparticle catalysts for their greater catalytic selectivity. The most common method for creating single-site catalysts involves anchoring the catalytically active moiety onto a surface. This approach unfortunately tends to create problems with uniformity and surface-catalyst interactions [44]. MOFs have been presented as a solution to these problems as they are crystalline (i.e., highly uniform)

materials and can be tuned with relative ease. Constraining catalytically active sites within MOFs can also prevent catalyst deactivation by ligand disproportionation. This type of functionalization leads to the formation of mixed-metal organic frameworks (M-MOFs). In this section, three methods for the functionalization of MOF clusters will be highlighted in regard to organometallic catalytic performance.

3.1. Post-Synthetic Metalation

Metals or organometallic species can be post-synthetically grafted onto a metal cluster. This technique is utilized when substitution within the cluster is not desired, but imparted functionality to the clusters is desired. Most often this technique is used to maintain structural stability in the framework where post-synthetic metal exchange (PSME) would result in structural instability or collapse. Post-synthetic metalation does not substitute metal atoms that already exist within the metal cluster, instead this technique grafts organometallic moieties onto the existing cluster in a structure. This approach can be accomplished through using techniques such as atomic layer deposition in MOFs (AIM) or through traditional organometallic chemical techniques. When considering the behavior of the organometallic moiety, the metal clusters in the scaffold can be treated as both a ligand and as a support.

3.1.1. Platforms Suitable for Post-Synthetic Metalation

Group IV clusters, primarily $[\text{Zr}_6(\mu_3\text{-O})_4(\mu_3\text{-OH})_4(\text{COO})_{12}]$ clusters (hereafter Zr_6 clusters), are the most common clusters used as supports for organometallic moieties. These clusters are common in MOFs, as they allow for high connectivity and are generally stable [45]. One of the earliest MOFs reported that contained a Group IV cluster was UiO-66. This structure contained 12-connected Zr_6 cluster joined by linear benzene dicarboxylate (bdc) linkers [46]. UiO-66 also has stable isostructural frameworks, UiO-67 and -68, which can be generated through isorecticular expansion of the organic ligands [46]. These MOFs have been extensively studied in the literature [46–50]. The Zr_6 cluster that is used in the UiO series has become perhaps the most popularly used Group IV cluster in MOF chemistry. A large number of Zr-MOFs: the PCN-700 series [51], NU-1000 (NU = Northwestern University) [52], MOF-545 [53], and NU-1200 [54], contain this cluster.

Zr-based clusters have several key advantages over other common clusters such as basic zinc carboxylates (BZCs) or paddlewheel clusters. Zr_6 clusters are tolerant to defects and can have high connectivity (up to 12 linkers) [45] compared to BZCs (up to 6 linkers) [55] or paddlewheel clusters (up to 4 linkers) [56]. This higher connectivity creates a greater degree of tunability for this structure as compared to lower connected clusters. In addition to the high connectivity, Zr_6 MOFs are also particularly stable due to their high cluster charge [45]. Although high connectivity is permitted by Zr_6 clusters, their tolerance to defects means that MOF variants with lower connectivity can also be designed without major loss to structural stability, which can lead to the presence of open coordination sites around the cluster that are available for post-synthetic metalation (Figure 4). In addition to the catalytic behavior and further functionalizability of the open coordination sites [57,58], coordinatively unsaturated metal clusters are also more likely to form flexible MOFs. This category of MOF is currently a hotbed for the study of selective or switchable catalysis [51,59]. Combining these properties with post-synthetic metalation of clusters creates exciting opportunities for the expansion of the range of reactions that can be catalyzed using Zr-MOFs.

3.1.2. Post-Synthetic Metalation Techniques

One commonly used technique for post-synthetic metalation is the use of AIM [60]. A famous example of the use of AIM in MOFs comes from the Hupp and Farha groups. In their work, they demonstrated the usability of NiS as a grafting material onto Zr_6 metal nodes in NU-1000 (Figure 5). In this method, nickel and sulfur precursors are vaporized and are deposited onto the MOF framework. The nickel binds to the hydroxyl/aqua ligand

pairs in the first deposition step, and sulfur binds to the nickel in the second step [60]. Interestingly, the nickel species deposited by AIM are not distributed evenly across the structure. Clusters of nickel in the NU-1000 modified material were shown to gather predominantly within the smaller pores of the NU-1000 structure [61]. Following the deposition of nickel sulfide, the material could be used for photocatalytic water splitting experiments. It was found that the parent NU-1000 framework could not perform water splitting, but the NiS@NU-1000 composite material was highly active, evolving a significant amount of H₂ [60]. In addition to Ni, other metals have also been deposited using AIM, including Mo, Nb, and Co [62–64].

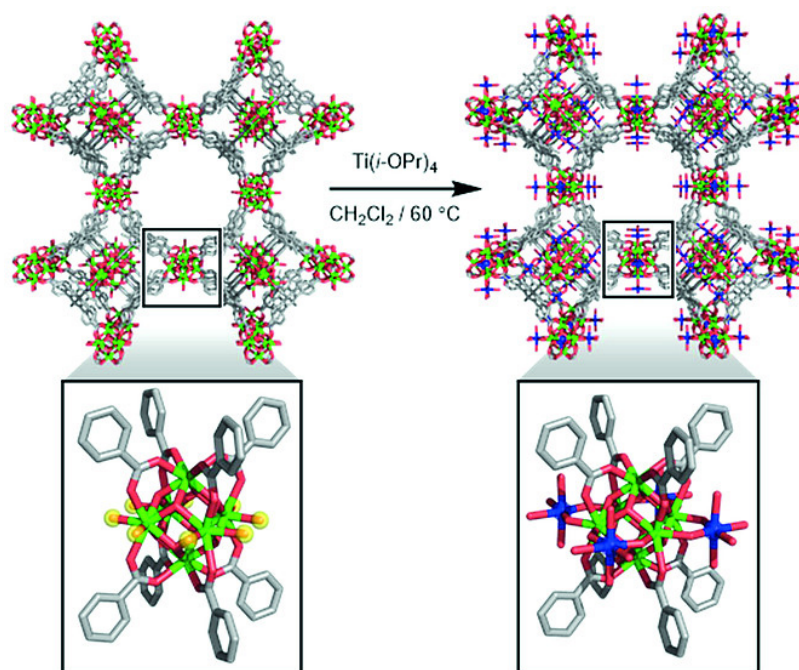


Figure 4. Synthetic scheme of Ti(IV) deposition on NU-1200, highlighting the exposed $\text{-OH/H}_2\text{O}$ groups of the Zr₆ cluster that are available to post-synthetic metalation. Green = Zr, Blue = Ti, Red = O, Gray = C. Adapted with permission from [54]; Published by WILEY, 2016.

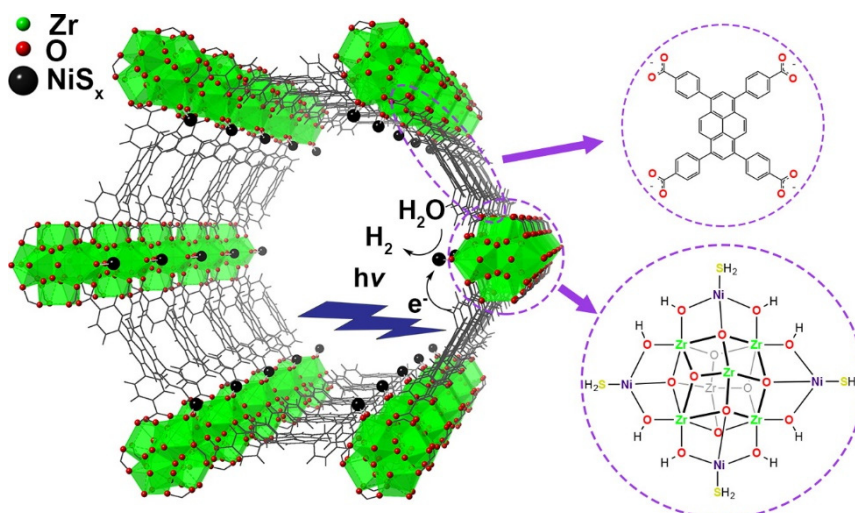


Figure 5. Idealized structure of NiS_x-functionalized NU-1000. The ligand and proposed structure of the atomic layer deposition in metal–organic frameworks (AIM)-metalated cluster are also shown. Green = Zr, Red = O, Black = NiS_x. Adapted with permission from [60]; Published by American Chemical Society, 2016.

An alternative to the utilization of the AIM strategy is through solution-phase metalation, sometimes referred to as solvent-assisted metal incorporation (SAMI) or solvothermal deposition in a MOF (SIM). In this technique, the preformed MOF is suspended in a solution of metal precursor for up to 24 h at relatively mild temperatures [54]. This technique is highly suited to stable Zr-MOFs, such as NU-1200 and NU-1000, as it is vital that the MOF be stable while suspended in solution at mildly elevated temperatures. As with AIM, metals are grafted onto the metal clusters via aqua/hydroxyl ligand pairs. A wide range of transition metals have been deposited on these two frameworks by Hupp, Farha, and Gagliardi, including Ti(IV), Mo(IV), Mo(VI), Nb(V), Co(II), and Cu(II) [62,65,66].

While a range of metal precursors can be used in SIM, a significant body of work uses with metal acetylacetonate species, due to their good solubility in organic solvents. In an early example of the versatility of this technique, the Farha, Hupp, and Nguyen groups functionalized UiO-66 with redox active V(V) ions. By treatment of UiO-66 with VO(acac)₂ (acac = acetylacetonate) in methanol, it was determined that V(V) ions could replace ~5% of the bdc linkers, binding through the -OH groups at the missing linker site [67]. While no crystal structures could be determined, the group proposed the binding mode for these compounds through a combination of NMR analysis of the digested MOF and the growth of additional peaks in an in situ DRIFTS spectrum. This functionalized MOF was then used to catalyze the oxidative dehydrogenation of cyclohexene [67]. Later work in the Gagliardi and Gates groups demonstrated the same principle utilized with vanadium for iridium complexes supported on the Zr₆ clusters of NU-1000 and UiO-66 [68]. Unlike the work from Farha, Hupp, and Nguyen, Gagliardi and Gates found that some of the ligands remained bound to the iridium center. No crystal structures were able to be determined for the iridium functionalization, however Gagliardi and Gates provided EXAFS (extended X-ray absorption fine structure) data with DFT (density-functional theory) calculations to assign the binding sites and modes of the iridium complexes. Later work demonstrated that these M-MOFs could be used as effective ethylene conversion catalysts [48].

Capitalizing on the principles outlined in the previous work in this field, several zirconium cluster systems as supports for earth-abundant transition metal catalysts have been investigated. One such example comes from the Lin group whose work primarily focused on post-synthetic metalation of the Zr₆ clusters in UiO-68. Deprotonation of the Zr₃(μ -OH) sites with *n*-BuLi and treatment with CoCl₂ or FeBr₂ resulted in a M-MOF in which cluster H atoms were replaced by an organometallic catalyst moiety. The heterometals were bound to one oxide moiety from the cluster, both oxygen atoms of an attached linker, and a single halide atom in a distorted tetrahedral geometry [44]. Metalation of other zirconium cluster nodes with cobalt through μ_2 and μ_3 oxide binding was also studied. In all cases, the zirconium nodes acted as tridentate ligands to the heterometal [69,70]. These M-MOFs had high catalytic activity towards a wide range of organic reactions including: hydrogenation, borylation, amination, and silylation [44,70,71]. This work has been expanded to consider alkali earth metal organometallic catalysts as well. In one such report of a UiO-69 structure, when the structure was treated with MgMe₂, highly decorated Zr₆ clusters could be achieved. While the MgMe bound to the clusters through deprotonated μ -OH moieties, the zirconium nodes here could also act as a monodentate ligand. This is because the coordination from the carboxylate functionality is very weak. After functionalization, the structure was demonstrated to maintain high activity for hydroboration and hydroamination catalytic reactions [70].

The Lin group later expanded their work to Ti-MOF cluster-based supports for cobalt catalysts. This work utilized the MIL-125 (MIL = Materials Institute Lavoisier) structure, which contains 12-connected Ti₈O₈(OH)₄(COO)₁₂ clusters. As with their previous work, it was demonstrated that deprotonation occurs at the μ -OH sites. Upon treatment of the structure with CoCl₂, insertion of a CoCl moiety into the center of the cluster was accomplished. Here the cobalt was bound through four μ -O moieties. An additional coordinated solvent molecule (THF, tetrahydrofuran) became bound to the cobalt center, creating a distorted octahedral geometry around the metal ion [72]. Upon treatment

with NaBEt_3H , the reductive elimination of hydrogen resulted in Co-mediated electron transfer from the hydride, causing two of the eight Ti^{IV} centers to be reduced to Ti^{III} . This mixed valence M-MOF was then used to catalyze the hydrogenation of arenes and heteroarenes [72].

3.2. Post-Synthetic Metal Exchange

The composition of the clusters themselves can also be modified after the initial synthesis of the MOF through PSME. In general, this technique allows the metal clusters within the scaffold to be modified by substitution of existing metal ions with a different metal ion. This approach is advantageous as it allows the MOF to acquire additional functionality or stability through such substitution [73–75]. The major difference between PSME and post-synthetic metalation (PSM) is that in PSME, the metal ions in the clusters are exchanged with newly introduced metal ions yielding no net change in the total number of metal ions in a cluster. This is in contrast to PSM where metal ions are added to a cluster, yielding a net change in the total number of metal ions in a cluster. In particular, the approach of PSME offers the ability to synthesize desired MOFs that are otherwise unable to be formed due to steric, electronic, or stability concerns during synthesis.

PSME refers to a range of techniques by which metal ions in a cluster are exchanged with a more active metal cation. Typically PSME is performed on clusters containing relatively inert metals, however, this technique is fairly versatile and can be performed on a wide range of metal clusters [76]. One of the earliest examples of PSME in the literature was in the replacement of cadmium(II) ions with lead(II) and lanthanide(III) ions in the anionic MOF $[(\text{Cd}_4\text{O})_3(\text{hett})_8]^{6-}$ (H_3hett = ethyl substituted truxene tricarboxylic acid). Complete substitution was achieved by soaking the preformed MOF in aqueous lead nitrate or a lanthanide salt solution for two days. The partial substitution for this exchange could be achieved using shorter reaction times. The single-crystal to single-crystal transformation for this system was demonstrated to be completely reversible under mild conditions [77].

An important advantage for PSME is that it can be used to generate MOFs which are unable to be synthesized in a particular topology. Recent work in the Volkmer and Dinca groups has shown the usability of PSME for zinc MOF metal substitutions. MFU-4l (MFU = metal–organic framework, Ulm University), a zinc MOF with five zinc(II) cations in the cluster, is of topological and catalytic interest, but cannot be synthesized in situ with other metals beyond zinc [73,78]. Despite being unable to directly synthesize the isostructural MOFs of MFU-4l with other metals, PSME can be accomplished for the peripheral zinc ions with titanium, chromium, and cobalt (Figure 6) [73,75,78]. Substitution of the zinc ions with more active heterometal ions increased the activity of the MOF for a variety of catalytic applications, including: CO oxidation, olefin polymerization, and olefin insertion [73].

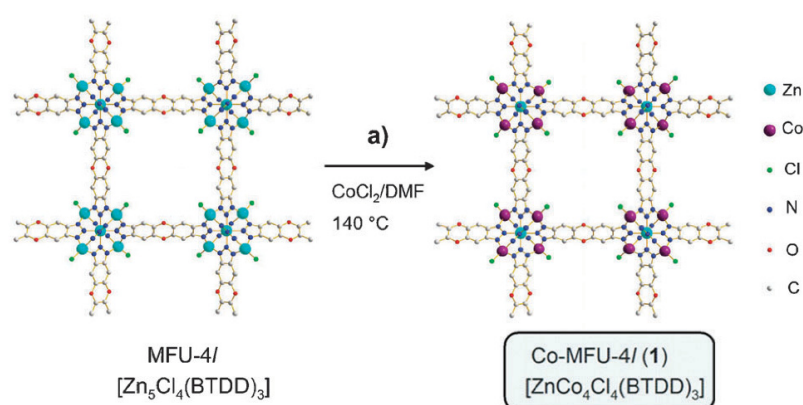


Figure 6. Structure and post-synthetic cobaltation of MFU-4. Turquoise = Zn, Maroon = Co, Green = Cl, Blue = N, Red = O, Gray = C. Adapted with permission from [78]; Published by Royal Society of Chemistry, 2012.

Similar to the work demonstrated in MFU-4l, substitution of inert nickel ions with active cobalt ions in Ni-MOF-74 has also been demonstrated. The resultant M-MOF demonstrated a higher catalytic conversion of cyclohexene than either pure Ni-MOF-74 or Co-MOF-74. This indicates the potential for high catalytic activity in M-MOFs in comparison to their homometallic MOF counterparts, per mole of active metal. It is believed that the increased catalytic activity demonstrated in this example stems from substitution of only the most accessible metal ions in the MOF [79].

PSME can also be utilized when the direct synthesis of a desired MOF cannot be accomplished in a predictable way. Titanium MOFs are highly desired as the titanium clusters within the MOF mimic the chemistry of titanium nanoparticles. Titanium is also a low toxicity earth abundant metal. Although titanium MOFs are highly desired for catalytic applications, it is often not possible to directly synthesize Ti-MOFs in a predictable way as the modulation techniques used for the analogous Zr- and Hf-MOFs do not work for titanium structures [45]. One highly accepted approach to the synthesis of Ti-MOFs is through the PSME of preformed Zr- or Hf-MOFs.

Cohen's group reported a total metal replacement of up to 38% of the Zr(IV) cations with Ti(IV) cations could be accomplished for UiO-66. The resulting structures retained the crystallinity of the original material, and have been shown to be both highly porous and stable [76]. However, a later study by the same group disproved this analysis, as scanning tunneling electron microscopy revealed that the Zr(IV) cations were not in fact substituted. Instead, a nanoscale TiO₂ layer was deposited on the surface of the particles, suggesting the exterior surface of the MOF was post synthetically metalated and that no cation exchange occurred. The Zr(IV) clusters in the interior of the crystal remained unaffected by the surface metalation and no zirconium was observed in the supernatant by ICP-MS (inductively coupled plasma mass spectrometry) following the supposed exchange [49].

Despite this setback, the Zhou group demonstrated that post-synthetic titanation is in fact possible and is not limited to substitution within preformed group IV MOFs. Their work demonstrated that replacement of metal ions such as scandium(III), zinc(II), and magnesium(II) with titanium(IV) in MOFs through the use of a Ti(III) intermediate can also be accomplished. By submersion of the preformed MOF in a Ti(III) rich solution, Ti(III) can be incorporated into the MOF structure and oxidized to yield Ti(IV). This can be accomplished without destroying the crystallinity or altering the overall structure of the parent MOF. However, judicious selection of the host MOF is crucial. The host MOF must be stable towards the Ti(III) intermediates, contain open metal sites and labile linkers to accelerate the metathesis, and contain a coordination site that will readily accommodate the substituted metal [80]. A similar technique has been used to replace magnesium with Fe(II) and Cr(II).

Other highly redox active metals such as iron(II/III) have also been investigated for PSME to improve the catalytic activity of the manganese(II) metal clusters. Using iron(III) chloride as an iron source, near complete substitution of manganese ions in Mn₃L₃ (H₂L = bis(4-(4'-carboxyphenyl)-3,5-dimethyl-pyrazolyl)methane) was performed [81]. M-MOFs containing smaller fractions of iron were also obtained by using shorter reaction times, lower temperatures, and alternative iron sources. The similarity between the parent Mn₃L₃ structure and the resulting M-MOF suggests that the iron incorporated in the structure is iron(II), despite coming from an iron(III) source. Most likely, the change in oxidation state is due to the original Mn clusters acting as a reductant [81].

3.3. In Situ Cation Doping

In situ cation doping is a less common, one-pot method for cationic substitution in MOFs as compared to post-synthetic methods. Utilizing this method, it is significantly more difficult to perform and direct the desired structure change in the M-MOF [82]. Cation doping generally involves partial substitution of the metal source with a heterometallic source. This strategy leads to a M-MOF in which the cations in the clusters are partially

substituted with the heterometallic cation. This approach can be utilized for a one-pot alteration of a parent MOF in regard to enhanced activity [83] or stability [82,84].

One well known example of in situ cation doping is exemplified in the Long group's work on iron-oxo species within MOFs. The Long group used a Fe-MOF for the conversion of ethane to ethanol using NO_2 under mild conditions. Although the iron sites are critical for the desired chemical conversion, it was necessary to substitute a large fraction (~95%) of the iron sites with redox-inactive magnesium ions. This was done to prevent oligomerization and overoxidation of the substrate. Rather than performing this substitution post-synthetically, the M-MOF was created by partial substitution of the iron source with a similar magnesium source during the solvothermal synthesis [83]. The oxidation state uniformity for the iron sites exhibited in the Mössbauer spectrum of the material indicated that the magnesium substitutions were distributed evenly throughout the structure. Although the final M-MOF was successful in catalyzing the oxidation of ethane to ethanol, it also suffered significant catalyst deactivation issues [83].

In situ cation doping has also been shown to be an effective technique for the increase in capture affinity of a desired substrate or to increase the stability of a desired MOF. In this work by the Shi and Cheng groups, MOF-5 was doped with either cobalt or nickel, demonstrating the improved H_2 uptake capabilities of each respective MOF as compared to the parent MOF-5 [84,85]. In addition to improving the uptake performance, it was also noted that for the heterometallic MOFs, the hydrostability of MOF-5 could be improved. A key drawback to MOF-5 is its instability, as the Zn-O bonds of MOF-5 and other related benzyl chloride MOFs can be hydrolyzed by atmospheric humidity [84,86–88]. While MOF-5 begins to degrade within two days of exposure to atmospheric humidity, Ni22-MOF-5 (22% Ni-doped) remained stable for more than one week (Figure 7) [84]. Ni-doped MOF-5 could also be combined with reduced graphene oxide in order to produce a high capacity energy storage composite material [82].

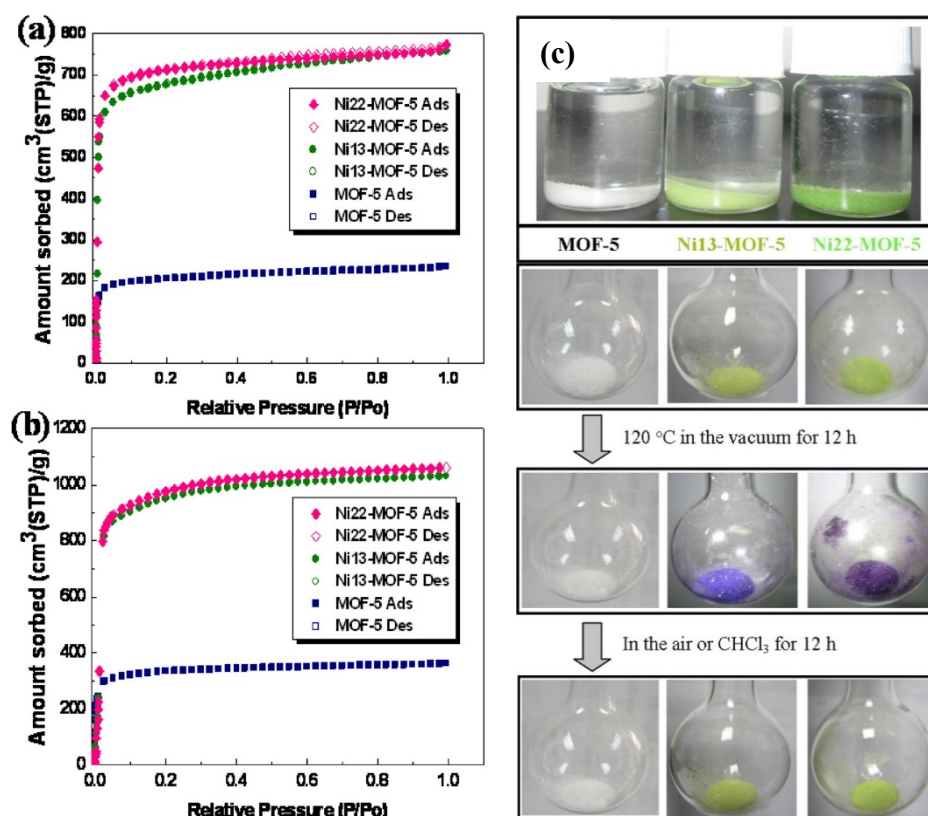


Figure 7. (a) N_2 and (b) Ar sorption isotherms of MOF-5 and Ni-doped MOF-5 with varying amounts of Ni; (c) color change of MOF-5 and Ni-doped MOF-5 under vacuum and re-exposure to air or CHCl_3 . Adapted with permission from [84]; Published by American Chemical Society, 2012.

4. Organometallic Catalysis in MOFs

One of the most important advances for the industrial scale production of chemicals is the incorporation of catalysts into chemical processes. By incorporating organometallic compounds, great developments in our modern world have taken place, particularly for oxidation, hydrogenation, C–H activation, and coupling reactions.

Although organometallic compounds have revolutionized the way we make and tailor chemical products, there are still some major drawbacks to organometallic compounds as catalysts for chemical processes. Many organometallic catalysts have limited lifetimes, which is most often caused by deactivation of the active site. Deactivation can occur through several pathways such as M–L redistribution, M–L oligomerization, and M–L conversion [89]. In addition, when used on an industrial scale, many organometallic catalysis are not recoverable from the reaction media as they are difficult to separate from the products in post-production. This decreases the overall economy of production.

The structure and tunability of MOFs provide a potential way to immobilize organometallic catalysts within the framework. This is advantageous as it increases both catalytic performance and the turnover number by protecting the catalyst. The added feature of the incorporation of heterogeneous catalysts within the framework also helps to prevent some common problems in homogeneous systems [90]. Here, we introduce several pieces of work that compare the performances of organometallic catalysts incorporated into MOFs to their free variants.

4.1. Reactions of Alkenes

Alkenes are very important chemicals for energy and chemical synthesis. Many important industrial alkene reactions, such as hydrogenation, oxidation, and isomerization reactions incorporate noble metals as catalysts [91,92]. For example, a catalyst that has been broadly incorporated into hydrogenation reactions for olefins, Wilkinson's catalyst, is Rh-based. Other noble metals, such as Pd have also been incorporated for olefin hydrogenation and oxidation reactions. These metal centers have been utilized on a large scale for alkene reactions but are very expensive and there is a limited quantity available. MOFs have been demonstrated to be highly efficient, size and conformationally selective catalysts even without the incorporation of noble metals as catalytic centers. The potential of utilizing MOFs as catalysts for reaction of alkenes is to take advantage of the properties of the material such as high specific surface areas, functionalized selectivity, and high gas sorption while also eliminating the need for noble metals in the catalytic conversion. Many of the reported works also realize highly efficient conversions of alkenes.

Site-isolation of the active sites within the MOF scaffold is crucial to keep active centers active for a prolonged lifetime. A recent example of this strategy was reported by the Lin group. In their work, TPHN-MOF-MgMe (TPHN = 4,4'-bis-(carboxyphenyl)-2-nitro-1,1'-biphenyl) was prepared by introducing MgMe sites onto the μ_3 -OH groups in TPHN-MOF's nodes (Figure 8). As a result of the well-separated Mg-species, the Schlenk-type ligand redistribution was successfully avoided. This MOF was then later successfully utilized for catalytic hydroboration of imines and hydroamination of amino alkenes under mild condition [93].

In addition to maintaining site activity, MOF scaffolds can be rationally designed to adjust the site specificity of the active-sites and inner structure. In this way, the framework can show improved performance as a kind of micro-reactor for chemical conversions. For instance, the Zhou group reported a one-step synthesis of a core-shell MOF, PCN-222(Fe)@Zr-BPDC (BPDC = biphenyl-4,4'-dicarboxylate), that enables the catalytic epoxidation of alkenes [94]. This hybrid core-shell structure was guided by differences in the nucleation rates of PCN-222's fast homogeneous nucleation and Zr-BPDC's accelerated heterogeneous nucleation. Its remarkable size-selectivity is studied through substrate expansion, which shows that the narrow open window will increase the diffusion resistance, thus block the reaction pathway for large-size alkenes like (Z/E)-1,2-diphenylethene. Moreover, Eddaoudi and co-workers successfully anchored $W(\equiv C^tBu)(CH_2^tBu)_3$ onto

Zr₆ clusters of NU-1000 [95]. The resulted material featured high catalytic properties in olefin metathesis.

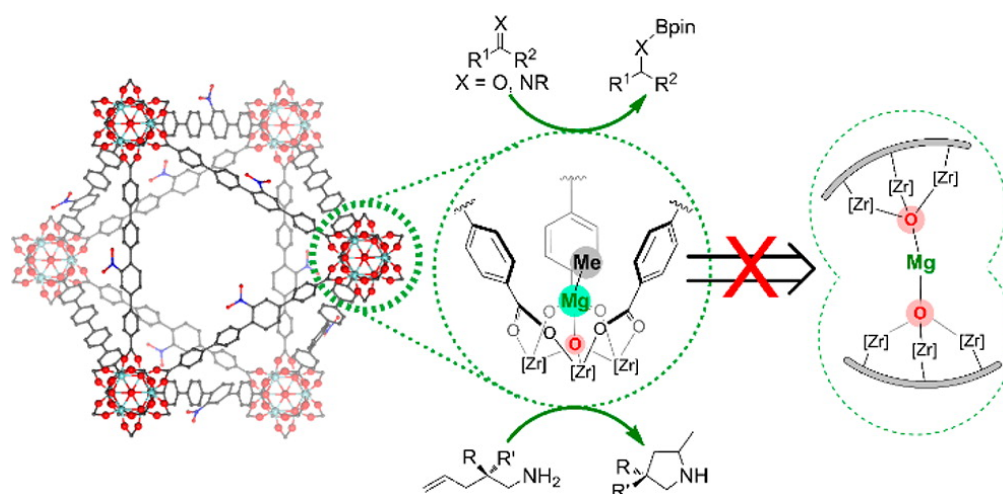


Figure 8. The site-isolation strategy of introducing MgMe sites as alkenes activation center. Red = O, Black = C, Blue = N, Green = Zr. Adapted with permission from [93]; Published by American Chemical Society, 2016.

In another study, trans-coordinate metal active sites were introduced into a MOF scaffold through sequential ligand elimination and installation. This trans-coordinate M-INA₂ (INA = 4-pyridinecarboxylate) MOF demonstrated higher activity in ethylene dimerization reactions over any known cis-binding MOF variant. [40] The trans-binding site approach, although higher in activity, is much more difficult to generate than a cis-binding site variant. A trans-coordinated site was synthetically accomplished using PCN-160 as a start material and simultaneously replacing the parent azobenzene-4,4'-dicarboxylate (AZDC) linkers with 4-carboxybenzylidene-4-aminobenzate (CBAB) linkers [96]. The CBAB linkers were then exchanged with M-INA₂ linkers. Through this multi-step ligand exchange, a MOF with trans-coordinated sites in the linkers was successfully synthesized. Neither a direct synthesis of the M-INA₂ containing PCN-160 or the exchange of the original AZDC ligands with M-INA₂ was unable to yield the desired MOF. The trans-chelated sites within this MOF demonstrated a significantly higher catalytic efficiency over the *cis*-binding sites previously demonstrated in any other MOF.

4.2. Pd-Catalyzed Cross-Coupling Reactions

Palladium-catalyzed cross-coupling reactions are considered to be one of the greatest breakthroughs in the field of organic chemistry in the modern era. This type of reaction is so important that in 2010 the Nobel Prize in Chemistry was awarded jointly to Drs. Richard F. Heck, Ei-ichi Negishi, and Akira Suzuki “for palladium-catalyzed cross coupling in organic synthesis.” This method is highly efficient for building carbon-carbon and carbon-nitrogen bonds directly, in high selectivity. These reactions also operate at relatively low temperatures and are often very high yielding [97].

After a long period of development, the usage of palladium-catalyzed coupling reactions to produce fine chemicals has significantly increased, but there are still some downsides of using the traditional catalytic protocols for industrial scale synthesis. For example, when performing the Heck coupling reaction, using ligands can prevent aggregation but it will make separation of the final products more difficult. If using palladium nanoparticles, the reaction will result in the catalyst precipitating after the reaction [98]. Immobilizing Pd species in MOF scaffolds can be utilized to transplant these Pd-catalyzed reactions into heterogeneous system [57].

NHC ligands can be utilized to fixate Pd catalysts within MOF scaffolds. One such example of this, reported by the Dong group, was in the case of Pd(II)-NHDC-UiO-67

(Figure 9). This MOF was developed for the catalytic Heck cross-coupling reaction of benzyne-benzyne-alkenes [99]. This approach demonstrated not only good catalytic efficiency for a broad range of substances, but also was highly recyclable. Another case of the NHC-MOF approach is in $\text{NH}_2\text{-MIL-101}(\text{Cr})$. In this work, the framework was utilized to catalyze Suzuki-Miyaura cross-coupling reactions for a variety of substrates [100]. There have also been reports of Pd incorporated MOFs that utilize other ligand beyond the NHC ligand approach. For example, the Li group reported a bpdc (para-biphenyldicarboxylate) ligand-based UiO-67 framework to immobilize Pd [101] and the Cohen group used a bpy ligand to chelate a Pd sites on the same parent skeleton [102]. Both approaches were shown to be versatile in that each could catalyze multiple Pd-catalyzed cross-coupling reactions.

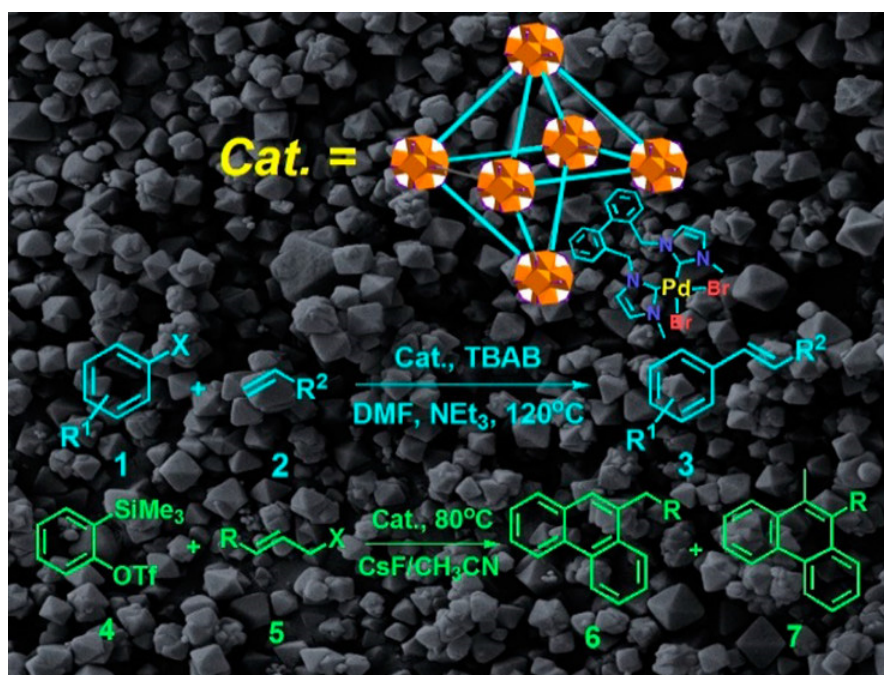


Figure 9. NHC (N-heterocyclic carbene) ligand bonded Pd sites in MOFs for Heck cross-coupling reaction. Orange = Zr-O clusters. Adapted with permission from [99]; Published by American Chemical Society, 2018.

An interesting application for Pd incorporated MOFs is in their use as sensors for Cu(II) ions, this application was first reported by the Jiang group [103]. In their work, they doped Pd sites into PCN-222 to form PCN-222-Pd(II) as a sensor. When copper ions were present in solution, the strong binding affinity of the porphyrin centers in the MOF readily replaced the Pd centers with Cu. The Pd ions were leached into the framework and were then reduced into nanoparticles. The PCN-222 framework was able to stabilize the nanoparticles which could be utilized as catalysts. The freshly generated Pd NPs were demonstrated to be efficient in catalytic *N*-Allyl-2-iodoaniline Heck cross-coupling reactions. The substrate was easily converted into 3-methylindole by the catalyst. As 3-methylindole has strong fluorescence, this system could be quantitative for the concentration of Cu(II) ions in solution [103].

4.3. C–H Activation Reactions

C–H activation reactions are chemical conversions that transform relatively inert C–H bonds into C–X bonds (X can be C, O, N and so on) [104]. These reactions have great value to petrochemical conversions as they can simplify the process of synthesizing desired chemicals from cruder starting materials [105]. The greatest challenge for these reactions involves the relatively high stability of saturated C–H bonds and the issue of selectivity [106].

Traditionally, there are three main approaches for C–H activation. The first approach to initiation is the removal of a hydrogen atom by using either a base, radical, or electrophile and subsequent attack of the active carbon atom. In the second approach an oxidative reaction is used to activate the carbon atom. This is the most widely used approach. In this approach, a metal atom inserts itself into the C–H bond to activate the carbon atom. The third approach for C–H activation is derived from metal-oxo enzyme chemistry. In this approach, a metal-oxo complex reacts with the hydrogen atom in the C–H bond forming a hydroxyl group. As a result, the carbon becomes activated [107]. Many of the reported work on C–H activation use organometallic compounds and are often second and third row transition metal-based. Metals such as Ru, Rh, Ir, and Pd are good candidates for the C–H active metal centers. The vast majority of these reactions are still performed in the homogeneous catalytic fashion [108]. As a result, it is feasible to assist in eliminating several common drawbacks while maintaining high performance of the active sites through using MOFs as the platform for this catalysis [109].

One example of the utilization of MOFs for C–H activation comes from the Lin group who reported the use of UiO-Co and UiO-Fe for C–H borylation, silylation, and amination in 2016 [70]. In their work it was observed that the reaction proceeded through deprotonation of $Zr_3(\mu_3\text{-OH})$ in the nodes of UiO-68 by $n\text{BuLi}$. The activated catalyst then reacted with a CoCl_2 or $\text{FeBr}_2 \cdot 2\text{THF}$ precursor, forming the active species $\mu_4\text{-O-M-H}$ ($M = \text{Co}$ or Fe) [44]. In the same year, the Lin group also reported a linker-based (mono)phosphine-M complex active site, $P_1\text{-MOF} \cdot M$ ($M = \text{Rh}$ and Ir), which was shown to catalyze the C–H borylation of arenes [110]. The active $M\text{-PR}_3$ complexes were able to be stabilized through the isolation of catalytic sites in the frameworks. Another approach published by the Zhou group (Figure 10) shows the possibility of postsynthetic incorporation of active sites into MOF's pores to realize C–H activation [111]. In this work an NNN-pincer-based PCN-308 MOF scaffold, synthesized from 4'-(4-carboxyphenyl)-[2,2':6',2''-terpyridine]-5,5''-dicarboxylic acid (H_3TPY) and Zr_6 clusters (Figure 10), was shown to be effective for C–H borylation reactions. This MOF had metal ions postsynthetically introduced to the pincer ligands forming highly active $M@PCN\text{-}308$, where $M = \text{Co}$ being exceptionally effective.

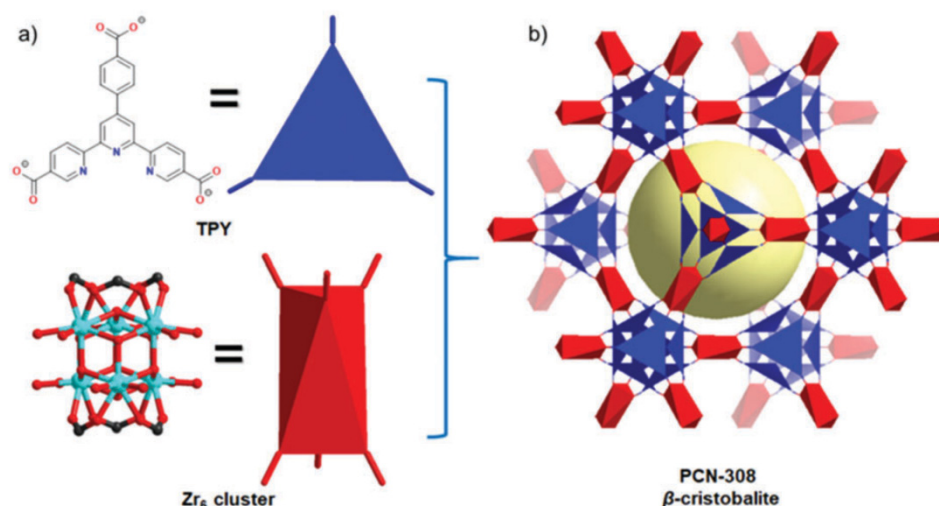


Figure 10. (a) Trigonally planar organic linker TPY and six-connected D_{3d} -symmetric Zr_6 antiprismatic clusters. (b) The β -Cristobalite network of PCN-308 simulated based on the reported PCN-777 structure. Blue = TPY ligand, Red = Zr_6 cluster, Yellow = void space. Adapted with permission from [111]; Published by Royal Society of Chemistry, 2019.

5. New Horizons to the Use of MOFs for Organometallic Transformations

Owing to their high tunability and versatile pore environments, MOFs are promising candidates for applications that require the incorporation of diverse function groups within highly ordered molecular systems [112]. The combination of utilizing organometallic

chemistry within the MOF frameworks can also introduce and improve the properties of MOFs for designer applications. In this section we will explore how the incorporation of organometallic chemistry into MOF frameworks can be utilized for real world applications beyond traditional organometallic applications. This work will only focus on gas sorption and separations, spin ordering in magnetism, and therapeutics, although there is a vast array of potential applications for these materials.

5.1. Gas Adsorption

In organometallics, metal centers with unsaturated coordination sites can possess high activities and strong interactions with specific gas molecules. For example, heme, the metal-porphyrin found in human blood and muscle tissue, contains a coordinately unsaturated Fe center. This Fe center is responsible for the controlled capture and release of O₂ in hemoglobin and myoglobin. The controlled binding and release of specific gases can also be applied in application-based design of MOFs. When the metal centers within the MOF framework are designed with open metal sites and their electronic environment is tailored to a specific selectivity, the metal sites can selectively and reversibly bind specific gas molecules. For instance, in 2014, the Harris group observed binding between O₂ and a four-coordinate ferrous center in a porphyrin-based MOF, PCN-224(Fe). Their study generated a superoxide Fe^{III}-porphyrin at −78 °C [113]. In later works, this system was be further extended to PCN-224(Mn) which also demonstrated selective reversible O₂ binding [114].

Moreover, through tuning the ligand environment and metal site electronics, MOFs with open metal sites can be synthesized to achieve selectivity for a desired gas. For instance, the Dincă group once observed NO disproportionation on an [FeZn₃O] center in a partial cation exchanged Fe²⁺-MOF-5 [115]. In 2015, the Long group reported a MOF, Fe₂(dobdc) (dobdc = 2,5-dioxido-1,4-benzenedicarboxylate), which contained coordinately unsaturated redox-active Fe²⁺ centers. Upon exposure to NO gas, a Fe₂(NO)₂(dobdc) species was formed [116]. This reversible binding involved the formation of Fe³⁺-NO[−] adducts, which could be tuned for the gradual release of NO gas. In another example from 2016, the Dincă group designed a series of MOFs, M₂Cl₂(BTDD)(H₂O)₂ (M = Mn, Co, Ni, BTDD = bis(1H-1,2,3-triazolo[4,5-b], [4',5'-i])dibenzo-[1,4]dioxin), that exhibited abundant, well-dispersed open metal sites with a highly selective uptake of NH₃ [117]. Building upon their previous work and that of the Dincă group, in 2017 the Long group reported two similar Fe-MOFs, Fe₂Cl₂(BTDD) and Fe₂Cl₂(BBTA) (BBTA = 1H,5H-benzo(1,2-d:4,5-d')bistriazole), containing unsaturated Fe^{II} centers (Figure 11) [118]. Upon exposure to CO, the neighboring Fe centers along the coordination chain underwent a high-spin to low-spin transition, leading to cooperative adsorption of CO with very low regeneration energies. The selective CO scavenging through the Fe binding site spin-state transition could also be observed in the MOF, Fe₃[(Fe₄Cl)₃(BTtri)₈]₂·18CH₃OH (BTtri = 1,3,5-tris(1H-1,2,3-triazol-5-yl)benzene) [119]. The Long group synthesized a MOF Fe₂(dobdc) (dobdc: 2,5-dioxido-1,4-benzenedicarboxylate) with open Fe(II) sites, which can coordinate with olefins reversibly [120]. These properties were applied in membrane-based separation of olefin/paraffin.

Remarkably, redox-active properties at the metal site can also be applied for the capture of gas molecules. Some low-valence metals can form reversible binding with oxidant gas to give a high valence, while the robustness of the frameworks can still be maintained. In 2017, the Dincă group generated a MOF with reversible binding between Co₂Cl₂(BTDD) and the elemental halogens Cl₂ and Br₂ [121]. In this system, the Co^{II} centers in the Co₂Cl₂(BTDD) MOF became oxidized by Cl₂ or Br₂ yielding a Co^{III} center. This process was quantitative and demonstrated the reversibility of the bond through the release of the halogen molecules while heating. A radical mechanism is proposed to explain the homolytic cleavage of the Co^{III}—X bond to give halogen elements.

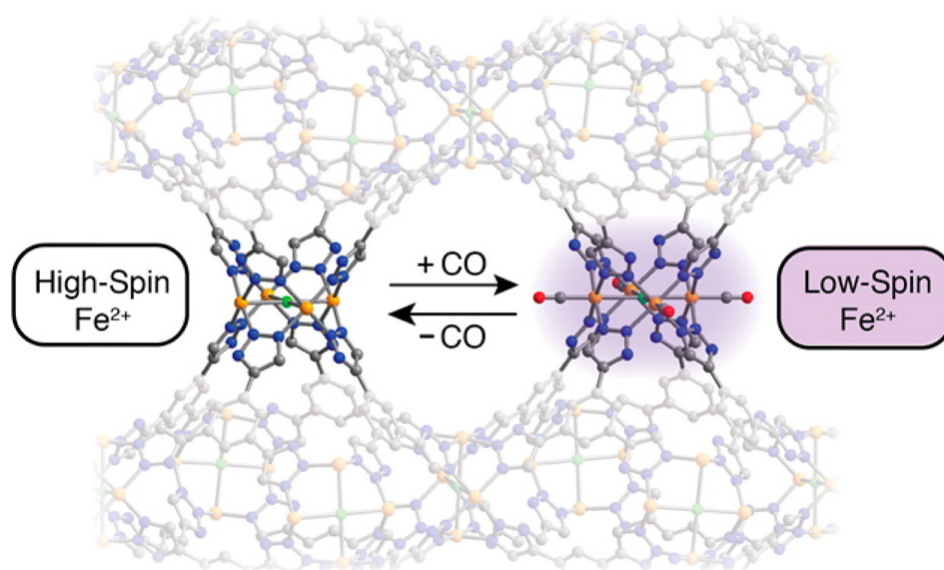


Figure 11. Reversible CO scavenging observed in MOF $\text{Fe}_3[(\text{Fe}_4\text{Cl})_3(\text{BTri})_8]_2 \cdot 18\text{CH}_3\text{OH}$ (BTri = 1,3,5-tris(1H-1,2,3-triazol-5-yl)benzene) driven by spin-state transition in Fe centers. Blue = N. Red = O. Yellow = Fe. Green = Cl. Grey = C. Adapted with permission from [119]; Published by American Chemical Society, 2016.

5.2. Magnetism

Magnetism is one of the primary properties of organometallic compounds and porous magnets have drawn great attention owing to their potential applications in high-density information storage. The low working temperatures of many magnets, including porous magnets, restrict their practical application. For instance, the record high ordering temperature of magnetic MOFs was only 32 K in 2014 [122]. It is usually contradictory to design a MOF with a high ordering temperatures and large surface area. This is because the super-exchange coupling between the paramagnetic centers decreases dramatically with increased distance between centers. While ligands typically used in MOF synthesis seem to be too long to give strong coupling between magnetic centers, some groups in recent years have reported cyan-functionalized ligands as possible solutions to this problem. In particular, TCNE and TCNQ (TCNE = tetracyanoethylene, TCNQ = 7,7,8,8-tetracyanoquinodimethane) have been used to construct network magnets with voids and high ordering temperatures. However, the weak coordination bonds between these ligands and the transition metal centers make it difficult to obtain robust permanent pores in the structures [123–125]. Such an issue had not been solved until 2015, when the Harris group utilized a semiquinoid ligand, 2,5-dichloro-3,6-dihydroxy-1,4-benzoquinone to synthesize a radical-bridging MOF, $(\text{Me}_2\text{NH}_2)_2[\text{Fe}_2\text{L}_3] \cdot 2\text{H}_2\text{O} \cdot 6\text{DMF}$ (DMF = dimethylformamide), that had an ordering temperature of 80 K and a BET surface area of $885 \text{ m}^2/\text{g}$ [126]. During the synthesis of this MOF, two thirds of the ligands could be reduced into a radical form. This unique property allowed for bridging between adjacent Fe^{III} centers through strong antiferromagnetic coupling. Further studies indicated that once the ligands were fully reduced to their radical form, the ordering temperature of the MOF could be increased to 105 K [127].

5.3. Quantum Computation

Qubits, objects existing in any quantum superpositions of two states, are the fundamental units of quantum information systems. An individual paramagnetic compound can be utilized as a qubit due to the diversity in spin states that can exist in many transition metal complexes. The spin can be tuned from a spin up to a spin down, or visa-versa, allowing for precise control of the qubit spin state. A spatial organization of qubits into an array is a promising strategy for the construction of quantum sensors and informa-

tion processing systems. Unfortunately, qubits have a downside. They are very sensitive to magnetic noise, ultimately impeding current development in this field. To overcome the barrier, in 2017, the Freedman group fabricated qubits into the framework of PCN-224 by mixing paramagnetic Co^{II} -porphyrin and diamagnetic Zn^{II} -porphyrin to achieve $[(\text{TCPP})\text{Co}_{0.07}\text{Zn}_{0.93}]_3[\text{Zr}_6\text{O}_4(\text{OH})_4(\text{H}_2\text{O})_6]_2$ [128]. The qubits in the framework exhibited a clock transition, thereby eliminating the influence of local magnetic noise, yielding a longer lifetime of 14 μs for the qubits (Figure 12). Building upon this work, in 2019, the same group constructed a PCN-224 framework that was fully substituted with Cu^{II} -porphyrin to achieve concise position control of the qubits [129]. In this system, a precise array of qubits, which were Cu^{II} sites on porphyrinic ligands, could be achieved by controlling the distances between Cu^{II} sites. This work not only showed that vibrational environments in the lattice could affect the spin dynamics of the qubits, but it also provided a pathway to construct qubit arrays precisely.

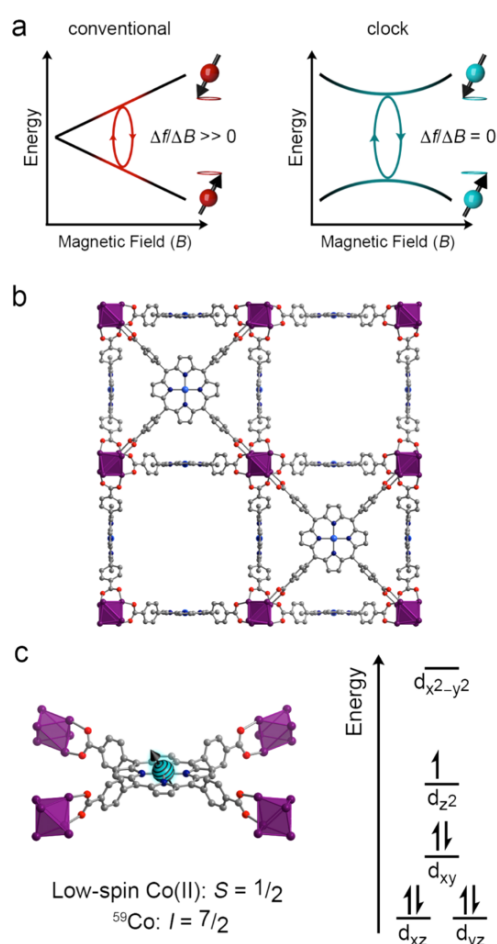


Figure 12. (a) Depiction of the clock concept for electronic spin qubits. Clock EPR transitions possess frequencies (f) that are insensitive to small changes in magnetic field (ΔB). This property may enable a long T_2 in magnetically noisy environments relative to a conventional EPR transition. (b) Crystal structure of the parent $[(\text{TCPP})\text{Co}]_3[\text{Zr}_6\text{O}_4(\text{OH})_4(\text{H}_2\text{O})_6]_2$ framework (TCPP = tetrakis(4-carboxyphenyl)-porphyrin) [128]. This material is porous, exhibiting a high surface area ($\sim 3200 \text{ m}^2/\text{g}$), and hosts paramagnetic cobalt(II) metal ions. (c) Close-up view of the square-planar cobalt(II) ions in the structure and qualitative depiction of the d-orbital splitting. The cobalt(II) ions are low-spin, featuring one unpaired electron that is strongly coupled to the $I = 7/2$ ^{59}Co nucleus. This strong hyperfine interaction engenders an avoided crossing such as that shown in (a). Purple = Zr. Cyan = Co. Grey = C. Red = O. Adapted with permission from [128]; Published by American Chemical Society, 2017.

5.4. Therapeutic

Numerous organometallic compounds have been shown to have a variety of applications in medicine. For example, cisplatin is an organometallic chemotherapy drug derived from platinum. Although many organometallic compounds are highly effective for medicinal applications, they are often difficult to direct to precise locations within the body, leading to unwanted side effects. Owing to intrinsic porosity and surface tunability, nanoscale MOFs can also serve as drug delivery agents to improve location targeting for an organometallic complex within the body. Some of the seminal work in this field came from the Lin group who has been working on a systematic study on this field. In 2009, they loaded a cisplatin prodrug, ethoxysuccinato-cisplatin (ESCP), onto NH_2 -BDC ligands of nanosized MIL-101(Fe) (NH_2 -BDC = 2-aminoterephthalic acid) [130]. The bonding between ESCP and NH_2 -BDC was quite labile causing a more gradual release of the ESCP. In 2014, the Lin group reported a successful loading of the cisplatin prodrug onto a Zr-MOF. The MOF@drug complex could be further coated with small interfering RNA, improving the chemotherapeutic efficacy [131].

Specific organometallic compounds can generate active agents to inhibit cancer cell growth. In 2018, Lin group constructed a cationic nanoscale MOF, Hf-DBB-Ru (DBB-Ru = bis(2,2'-bipyridine)(5,5'-di(4-benzoato)-2,2'-bipyridine)-ruthenium(II) chloride), that featured a high mitochondrial targeting ability. In their study, it was found that DBB-Ru could generate singlet oxygen and the Hf clusters could produce hydroxyl radicals once exposed to X-ray during radiodynamic therapy and radiotherapy [132]. Such a strategy was further extended to Hf-MOFs loaded with photosensitive $\text{Ir}(\text{bpy})[\text{dF}(\text{CF}_3)\text{ppy}]_2^+$ ligands. This combination within the scaffold yielded instant and reproductive death of tumor cells even at a modest X-ray dose (Figure 13) [133]. In another example, the Furukawa group installed metal carbonyl ligands onto UiO-67, achieving CORF-1, $\text{MnBr}(\text{bpydc})(\text{CO})_3@ \text{UiO}-67$ (bpydc = 5,5'-dicarboxylate-2,2'-bipyridine). CORF-1 was demonstrated to be able to release CO under exposure to light and have great potential in therapy for several inflammatory diseases [134].

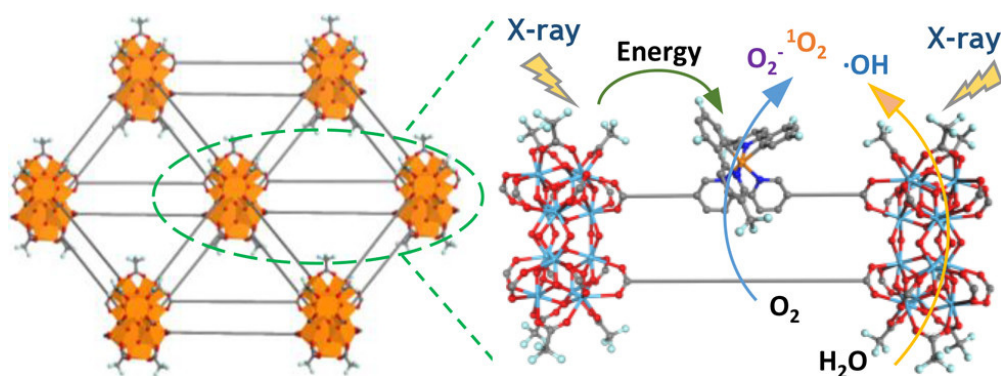


Figure 13. A combination of Hf_{12} cluster and photosensitive ligand featuring enhanced behavior in radiotherapy and radiodynamic therapy. Orange = Hf-oxo clusters. Red = O. Cyan = Hf. Blue = N. Green = F. Grey = C. Adapted with permission from [133]; Published by American Chemical Society, 2018.

6. Conclusions

The purpose of this review is to showcase the ultra-high tunability, versatility, and originality of MOFs as a next-generation approach to organometallic catalytic processes. Due to the structural features and diverse utility of these structures, MOFs are emerging as premier catalytic systems for the chemical transformations of materials traditionally only converted using organometallic catalysts. From the linkers within the frameworks, we are able to design specific catalytic reactions for site-isolated catalysts with constrained systems not possible in traditional directions. These features offer a unique study of the impacts of ligand steric hindrance effects as well as the influences of electronics of

catalytic metal centers. The metal center functionalization offers a unique approach to the tunability of a system towards desired chemical outcomes. As a result, both ligand-based and metal cluster-based studies have aided in the development of MOF centered organometallic chemical processes. As new and diverse structures of MOFs are developed, a greater understanding of the potential applications of these systems becomes available. MOFs offer a promising alternative for an even brighter future through their utilization in organometallic chemical processes. We expect that given the relative infancy of this field to that of catalytic chemical transformations, we will see many new approaches to this important area of research in the foreseeable future.

Author Contributions: Conceptualization, H.F.D., L.F., H.-C.Z.; writing—original draft preparation, F.C., J.A.P., K.-Y.W., T.-H.Y., H.F.D.; writing—reviewing and editing, F.C., H.F.D., L.F.; visualization, K.-Y.W.; supervision, H.-C.Z.; project administration, H.F.D., F.C.; funding acquisition, H.-C.Z. All authors have read and agreed to the published version of the manuscript.

Funding: This work was supported by the Robert A. Welch Foundation through a Welch Endowed Chair to H.-C.Z. (A-0030).

Data Availability Statement: Data sharing not applicable.

Acknowledgments: The authors acknowledge the financial supports of Robert A. Welch Foundation through a Welch Endowed Chair to H.-C.Z. (A-0030).

Conflicts of Interest: The authors declare no conflict of interest.

References

- Whitesides, G.M. Reinventing chemistry. *Angew. Chem. Int. Ed.* **2015**, *54*, 3196–3209. [[CrossRef](#)] [[PubMed](#)]
- Barnaby, R.; Liefeld, A.; Jackson, B.P.; Hampton, T.H.; Stanton, B.A. Effectiveness of table top water pitcher filters to remove arsenic from drinking water. *Environ. Res.* **2017**, *158*, 610–615. [[CrossRef](#)] [[PubMed](#)]
- Benavides, P.T.; Sun, P.; Han, J.; Dunn, J.B.; Wang, M. Life-cycle analysis of fuels from post-use non-recycled plastics. *Fuel* **2017**, *203*, 11–22. [[CrossRef](#)]
- Phalke, V.S.; Arote, A.P.; Sonawane, R.R. Design and development of machine which generates fuel using pyrolysis of waste plastic. *Int. J. Sci. Res. Dev.* **2017**, *5*, 1–6.
- Li, H.; Eddaoudi, M.; Groy, T.L.; Yaghi, O.M. Establishing microporosity in open metal-organic frameworks: Gas sorption isotherms for Zn(BDC) (BDC = 1,4-benzenedicarboxylate). *J. Am. Chem. Soc.* **1998**, *120*, 8571–8572. [[CrossRef](#)]
- Yaghi, O.M.; Li, G.; Li, H. Selective binding and removal of guests in a microporous metal-organic framework. *Nature* **1995**, *378*, 703–706. [[CrossRef](#)]
- Kirchon, A.; Feng, L.; Drake, H.F.; Joseph, E.A.; Zhou, H.-C. From fundamentals to applications: A toolbox for robust and multifunctional MOF materials. *Chem. Soc. Rev.* **2018**, *47*, 8611–8638. [[CrossRef](#)]
- Dhakshinamoorthy, A.; Garcia, H. Metal-organic frameworks as solid catalysts for the synthesis of nitrogen-containing heterocycles. *Chem. Soc. Rev.* **2014**, *43*, 5750–5765. [[CrossRef](#)] [[PubMed](#)]
- Dhakshinamoorthy, A.; Santiago-Portillo, A.; Asiri, A.M.; Garcia, H. Engineering UiO-66 metal organic framework for heterogeneous catalysis. *ChemCatChem* **2019**, *11*, 899–923. [[CrossRef](#)]
- Dhakshinamoorthy, A.; Asiri, A.M.; Garcia, H. Metal organic frameworks as multifunctional solid catalysts. *Trends Chem.* **2020**, *2*, 454–466. [[CrossRef](#)]
- Dincă, M.; Gabbaï, F.P.; Long, J.R. Organometallic chemistry within metal-organic frameworks. *Organometallics* **2019**, *38*, 3389–3391. [[CrossRef](#)]
- An, B.; Zeng, L.Z.; Jia, M.; Li, Z.; Lin, Z.K.; Song, Y.; Zhou, Y.; Cheng, J.; Wang, C.; Lin, W.B. Molecular iridium complexes in metal-organic frameworks catalyze CO₂ hydrogenation via concerted proton and hydride transfer. *J. Am. Chem. Soc.* **2017**, *139*, 17747–17750. [[CrossRef](#)] [[PubMed](#)]
- Bai, Y.; Dou, Y.; Xie, L.-H.; Rutledge, W.; Li, J.-R.; Zhou, H.-C. Zr-based metal-organic frameworks: Design, synthesis, structure, and applications. *Chem. Soc. Rev.* **2016**, *45*, 2327–2367. [[CrossRef](#)] [[PubMed](#)]
- Bosch, M.; Yuan, S.; Rutledge, W.; Zhou, H.-C. Stepwise synthesis of metal-organic frameworks. *Acc. Chem. Res.* **2017**, *50*, 857–865. [[CrossRef](#)]
- Burgess, S.A.; Kassie, A.; Baranowski, S.A.; Fritzsche, K.J.; Schmidt-Rohr, K.; Brown, C.M.; Wade, C.R. Improved catalytic activity and stability of a palladium pincer complex by incorporation into a metal-organic framework. *J. Am. Chem. Soc.* **2016**, *138*, 1780–1783. [[CrossRef](#)] [[PubMed](#)]
- Cui, Y.; Li, B.; He, H.; Zhou, W.; Chen, B.; Qian, G. Metal-organic frameworks as platforms for functional materials. *Acc. Chem. Res.* **2016**, *49*, 483–493. [[CrossRef](#)]
- Zhou, H.C.; Long, J.R.; Yaghi, O.M. Introduction to metal-organic frameworks. *Chem. Rev.* **2012**, *112*, 673–674. [[CrossRef](#)]

18. Ji, Z.; Wang, H.; Canossa, S.; Wuttke, S.; Yaghi, O.M. Pore chemistry of metal–organic frameworks. *Adv. Funct. Mater.* **2020**, *30*, 2000238. [\[CrossRef\]](#)
19. Kreno, L.E.; Leong, K.; Farha, O.K.; Allendorf, M.; Van Duyne, R.P.; Hupp, J.T. Metal-organic framework materials as chemical sensors. *Chem. Rev.* **2012**, *112*, 1105–1125. [\[CrossRef\]](#) [\[PubMed\]](#)
20. Lee, J.; Farha, O.K.; Roberts, J.; Scheidt, K.A.; Nguyen, S.T.; Hupp, J.T. Metal-organic framework materials as catalysts. *Chem. Soc. Rev.* **2009**, *38*, 1450–1459. [\[CrossRef\]](#)
21. Li, J.R.; Sculley, J.; Zhou, H.C. Metal-organic frameworks for separations. *Chem. Rev.* **2012**, *112*, 869–932. [\[CrossRef\]](#) [\[PubMed\]](#)
22. Nath, I.; Chakraborty, J.; Verpoort, F. Metal organic frameworks mimicking natural enzymes: A structural and functional analogy. *Chem. Soc. Rev.* **2016**, *45*, 4127–4170. [\[CrossRef\]](#)
23. Zhang, Y.M.; Yuan, S.; Day, G.; Wang, X.; Yang, X.Y.; Zhou, H.C. Luminescent sensors based on metal-organic frameworks. *Coord. Chem. Rev.* **2018**, *354*, 28–45. [\[CrossRef\]](#)
24. Furukawa, H.; Cordova, K.E.; O’Keeffe, M.; Yaghi, O.M. The chemistry and applications of metal-organic frameworks. *Science* **2013**, *341*, 974. [\[CrossRef\]](#) [\[PubMed\]](#)
25. Zhang, Y.M.; Yang, X.Y.; Zhou, H.C. Synthesis of MOFs for heterogeneous catalysis via linker design. *Polyhedron* **2018**, *154*, 189–201. [\[CrossRef\]](#)
26. Zhao, M.; Ou, S.; Wu, C.D. Porous Metal-organic frameworks for heterogeneous biomimetic catalysis. *Acc. Chem. Res.* **2014**, *47*, 1199–1207. [\[CrossRef\]](#)
27. Gao, W.Y.; Chrzanowski, M.; Ma, S.Q. Metal-metalloporphyrin frameworks: A resurging class of functional materials. *Chem. Soc. Rev.* **2014**, *43*, 5841–5866. [\[CrossRef\]](#) [\[PubMed\]](#)
28. Feng, D.W.; Chung, W.C.; Wei, Z.W.; Gu, Z.Y.; Jiang, H.L.; Chen, Y.P.; Darensbourg, D.J.; Zhou, H.C. Construction of ultrastable porphyrin zirconium metal-organic frameworks through linker elimination. *J. Am. Chem. Soc.* **2013**, *135*, 17105–17110. [\[CrossRef\]](#)
29. Huang, N.; Yuan, S.; Drake, H.; Yang, X.Y.; Pang, J.D.; Qin, J.S.; Li, J.L.; Zhang, Y.M.; Wang, Q.; Jiang, D.L.; et al. Systematic engineering of single substitution in zirconium metal-organic frameworks toward high-performance catalysis. *J. Am. Chem. Soc.* **2017**, *139*, 18590–18597. [\[CrossRef\]](#) [\[PubMed\]](#)
30. Fateeva, A.; Chater, P.A.; Ireland, C.P.; Tahir, A.A.; Khimyak, Y.Z.; Wiper, P.V.; Darwent, J.R.; Rosseinsky, M.J. A water-stable porphyrin-based metal-organic framework active for visible-light photocatalysis. *Angew. Chem. Int. Ed.* **2012**, *51*, 7440–7444. [\[CrossRef\]](#)
31. Feng, D.W.; Gu, Z.Y.; Chen, Y.P.; Park, J.; Wei, Z.W.; Sun, Y.J.; Bosch, M.; Yuan, S.; Zhou, H.C. A highly stable porphyrinic zirconium metal-organic framework with shp-a topology. *J. Am. Chem. Soc.* **2014**, *136*, 17714–17717. [\[CrossRef\]](#)
32. Huang, N.; Wang, K.C.; Drake, H.; Cai, P.Y.; Pang, J.D.; Li, J.L.; Che, S.; Huang, L.; Wang, Q.; Zhou, H.C. Tailor-made pyrazolide-based metal-organic frameworks for selective catalysis. *J. Am. Chem. Soc.* **2018**, *140*, 6383–6390. [\[CrossRef\]](#) [\[PubMed\]](#)
33. Wang, C.; Xie, Z.G.; deKrafft, K.E.; Lin, W.L. Doping Metal-organic frameworks for water oxidation, carbon dioxide reduction, and organic photocatalysis. *J. Am. Chem. Soc.* **2011**, *133*, 13445–13454. [\[CrossRef\]](#)
34. Zhu, Y.Y.; Lan, G.X.; Fan, Y.J.; Veroneau, S.S.; Song, Y.; Micheroni, D.; Lin, W.B. Merging photoredox and organometallic catalysts in a metal-organic framework significantly boosts photocatalytic activities. *Angew. Chem. Int. Ed.* **2018**, *57*, 14090–14094. [\[CrossRef\]](#) [\[PubMed\]](#)
35. Lan, G.X.; Li, Z.; Veroneau, S.S.; Zhu, Y.Y.; Xu, Z.W.; Wang, C.; Lin, W.B. Photosensitizing metal-organic layers for efficient sunlight-driven carbon dioxide reduction. *J. Am. Chem. Soc.* **2018**, *140*, 12369–12373. [\[CrossRef\]](#) [\[PubMed\]](#)
36. Elumalai, P.; Mamlouk, H.; Yiming, W.; Feng, L.; Yuan, S.; Zhou, H.C.; Madrahimov, S.T. Recyclable and reusable heteroleptic nickel catalyst immobilized on metal-organic framework for suzuki-miyaura coupling. *ACS Appl. Mater. Interfaces* **2018**, *10*, 41431–41438. [\[CrossRef\]](#) [\[PubMed\]](#)
37. Lv, X.-L.; Wang, K.; Wang, B.; Su, J.; Zou, X.; Xie, Y.; Li, J.-R.; Zhou, H.-C. A base-resistant metalloporphyrin metal-organic framework for C-H bond halogenation. *J. Am. Chem. Soc.* **2017**, *139*, 211–217. [\[CrossRef\]](#)
38. Sikma, R.E.; Kunal, P.; Dunning, S.G.; Reynolds, J.E.; Lee, J.S.; Chang, J.S.; Humphrey, S.M. Organoarsine metal-organic framework with cis-diarsine pockets for the installation of uniquely confined metal complexes. *J. Am. Chem. Soc.* **2018**, *140*, 9806–9809. [\[CrossRef\]](#)
39. Yuan, S.; Qin, J.S.; Su, J.; Li, B.; Li, J.L.; Chen, W.M.; Drake, H.F.; Zhang, P.; Yuan, D.Q.; Zuo, J.L.; et al. Sequential transformation of zirconium(IV)-MOFs into heterobimetallic MOFs bearing magnetic anisotropic cobalt(II) centers. *Angew. Chem. Int. Ed.* **2018**, *57*, 12578–12583. [\[CrossRef\]](#)
40. Yuan, S.; Zhang, P.; Zhang, L.L.; Garcia-Esparza, A.T.; Sokaras, D.; Qin, J.S.; Feng, L.; Day, G.S.; Chen, W.M.; Drake, H.F.; et al. Exposed equatorial positions of metal centers via sequential ligand elimination and installation in MOFs. *J. Am. Chem. Soc.* **2018**, *140*, 10814–10819. [\[CrossRef\]](#)
41. Kosanovich, A.J.; Komatsu, C.H.; Bhuvanesh, N.; Ozerov, O.V.; Perez, L.M. Dearomatization of the PCP pincer ligand in a Re(V) oxo complex. *Chem. Eur. J.* **2018**, *24*, 13754–13757. [\[CrossRef\]](#) [\[PubMed\]](#)
42. He, J.P.; Waggoner, N.W.; Dunning, S.G.; Steiner, A.; Lynch, V.M.; Humphrey, S.M. A PCP Pincer Ligand for coordination polymers with versatile chemical reactivity: Selective activation of CO₂ gas over CO Gas in the solid state. *Angew. Chem. Int. Ed.* **2016**, *55*, 12351–12355. [\[CrossRef\]](#) [\[PubMed\]](#)
43. Carson, F.; Martinez-Castro, E.; Marcos, R.; Miera, G.G.; Jansson, K.; Zou, X.D.; Martin-Matute, B. Effect of the functionalisation route on a Zr-MOF with an Ir-NHC complex for catalysis. *Chem. Commun.* **2015**, *51*, 10864–10867. [\[CrossRef\]](#) [\[PubMed\]](#)

44. Manna, K.; Ji, P.; Lin, Z.; Greene, F.X.; Urban, A.; Thacker, N.C.; Lin, W. Chemoselective single-site Earth-abundant metal catalysts at metal–organic framework nodes. *Nat. Commun.* **2016**, *7*, 12610. [[CrossRef](#)] [[PubMed](#)]
45. Yuan, S.; Qin, J.S.; Lollar, C.T.; Zhou, H.C. Stable Metal-organic frameworks with group 4 metals: Current status and trends. *ACS Cent. Sci.* **2018**, *4*, 440–450. [[CrossRef](#)]
46. Cavka, J.H.; Jakobsen, S.; Olsbye, U.; Guillou, N.; Lamberti, C.; Bordiga, S.; Lillerud, K.P. A new zirconium inorganic building brick forming metal organic frameworks with exceptional stability. *J. Am. Chem. Soc.* **2008**, *130*, 13850–13851. [[CrossRef](#)]
47. Schaate, A.; Roy, P.; Godt, A.; Lippke, J.; Waltz, F.; Wiebcke, M.; Behrens, P. Modulated synthesis of Zr-based metal-organic frameworks: From nano to single crystals. *Chem. Eur. J.* **2011**, *17*, 6643–6651. [[CrossRef](#)]
48. Yang, D.; Odoh, S.O.; Borycz, J.; Wang, T.C.; Farha, O.K.; Hupp, J.T.; Cramer, C.J.; Gagliardi, L.; Gates, B.C. Tuning Zr₆ metal–organic framework (MOF) nodes as catalyst supports: Site densities and electron-donor properties influence molecular iridium complexes as ethylene conversion catalysts. *ACS Catal.* **2016**, *6*, 235–247. [[CrossRef](#)]
49. Denny, M.S.; Parent, L.R.; Patterson, J.P.; Meena, S.K.; Pham, H.; Abellan, P.; Ramasse, Q.M.; Paesani, F.; Gianneschi, N.C.; Cohen, S.M. Transmission electron microscopy reveals deposition of metal oxide coatings onto metal–organic frameworks. *J. Am. Chem. Soc.* **2018**, *140*, 1348–1357. [[CrossRef](#)]
50. Liu, L.; Chen, Z.; Wang, J.; Zhang, D.; Zhu, Y.; Ling, S.; Huang, K.-W.; Belmabkhout, Y.; Adil, K.; Zhang, Y.; et al. Imaging defects and their evolution in a metal-organic framework at sub-unit-cell resolution. *Nat. Chem.* **2019**, *11*, 622–628. [[CrossRef](#)]
51. Yuan, S.; Zou, L.; Li, H.; Chen, Y.-P.; Qin, J.; Zhang, Q.; Lu, W.; Hall, M.B.; Zhou, H.-C. Flexible zirconium metal-organic frameworks as bioinspired switchable catalysts. *Angew. Chem. Int. Ed.* **2016**, *55*, 10776–10780. [[CrossRef](#)]
52. Wang, T.C.; Vermeulen, N.A.; Kim, I.S.; Martinson, A.B.F.; Stoddart, J.F.; Hupp, J.T.; Farha, O.K. Scalable synthesis and post-modification of a mesoporous metal-organic framework called NU-1000. *Nat. Protoc.* **2015**, *11*, 149. [[CrossRef](#)]
53. Morris, W.; Voloskiy, B.; Demir, S.; Gandara, F.; McGrier, P.L.; Furukawa, H.; Cascio, D.; Stoddart, J.F.; Yaghi, O.M. Synthesis, structure, and metalation of two new highly porous zirconium metal-organic frameworks. *Inorg. Chem.* **2012**, *51*, 6443–6445. [[CrossRef](#)]
54. Liu, T.-F.; Vermeulen, N.A.; Howarth, A.J.; Li, P.; Sarjeant, A.A.; Hupp, J.T.; Farha, O.K. Adding to the arsenal of zirconium-based metal–organic frameworks: The topology as a platform for solvent-assisted metal incorporation. *Eur. J. Inorg. Chem.* **2016**, *2016*, 4349–4352. [[CrossRef](#)]
55. Clegg, W.; Harbron, D.R.; Homan, C.D.; Hunt, P.A.; Little, I.R.; Straughan, B.P. Crystal structures of three basic zinc carboxylates together with infrared and FAB mass spectrometry studies in solution. *Inorg. Chim. Acta* **1991**, *186*, 51–60. [[CrossRef](#)]
56. Köberl, M.; Cokoja, M.; Herrmann, W.A.; Kühn, F.E. From molecules to materials: Molecular paddle-wheel synthons of macromolecules, cage compounds and metal–organic frameworks. *Dalton Trans.* **2011**, *40*, 6834–6859. [[CrossRef](#)] [[PubMed](#)]
57. Corma, A.; García, H.; Llabrés i Xamena, F.X. Engineering Metal organic frameworks for heterogeneous catalysis. *Chem. Rev.* **2010**, *110*, 4606–4655. [[CrossRef](#)] [[PubMed](#)]
58. Yuan, S.; Lu, W.; Chen, Y.-P.; Zhang, Q.; Liu, T.-F.; Feng, D.; Wang, X.; Qin, J.; Zhou, H.-C. Sequential linker installation: Precise placement of functional groups in multivariate metal–organic frameworks. *J. Am. Chem. Soc.* **2015**, *137*, 3177–3180. [[CrossRef](#)]
59. Zhang, Y.; Zhang, X.; Lyu, J.; Otake, K.I.; Wang, X.; Redfern, L.R.; Malliakas, C.D.; Li, Z.; Islamoglu, T.; Wang, B.; et al. A flexible metal-organic framework with 4-connected Zr₆ nodes. *J. Am. Chem. Soc.* **2018**, *140*, 11179–11183. [[CrossRef](#)] [[PubMed](#)]
60. Peters, A.W.; Li, Z.; Farha, O.K.; Hupp, J.T. Toward inexpensive photocatalytic hydrogen evolution: A nickel sulfide catalyst supported on a high-stability metal–organic framework. *ACS Appl. Mater. Interfaces* **2016**, *8*, 20675–20681. [[CrossRef](#)] [[PubMed](#)]
61. Platero-Prats, A.E.; League, A.B.; Bernales, V.; Ye, J.; Gallington, L.C.; Vjunov, A.; Schweitzer, N.M.; Li, Z.; Zheng, J.; Mehdi, B.L.; et al. Bridging zirconia nodes within a metal–organic framework via catalytic ni-hydroxo clusters to form heterobimetallic nanowires. *J. Am. Chem. Soc.* **2017**, *139*, 10410–10418. [[CrossRef](#)]
62. Noh, H.; Cui, Y.; Peters, A.W.; Pahls, D.R.; Ortuño, M.A.; Vermeulen, N.A.; Cramer, C.J.; Gagliardi, L.; Hupp, J.T.; Farha, O.K. An exceptionally stable metal–organic framework supported molybdenum(vi) oxide catalyst for cyclohexene epoxidation. *J. Am. Chem. Soc.* **2016**, *138*, 14720–14726. [[CrossRef](#)] [[PubMed](#)]
63. Ahn, S.; Thornburg, N.E.; Li, Z.; Wang, T.C.; Gallington, L.C.; Chapman, K.W.; Notestein, J.M.; Hupp, J.T.; Farha, O.K. Stable Metal–organic framework-supported niobium catalysts. *Inorg. Chem.* **2016**, *55*, 11954–11961. [[CrossRef](#)]
64. Li, Z.; Peters, A.W.; Bernales, V.; Ortuño, M.A.; Schweitzer, N.M.; DeStefano, M.R.; Gallington, L.C.; Platero-Prats, A.E.; Chapman, K.W.; Cramer, C.J.; et al. Metal–organic framework supported cobalt catalysts for the oxidative dehydrogenation of propane at low temperature. *ACS Cent. Sci.* **2017**, *3*, 31–38. [[CrossRef](#)] [[PubMed](#)]
65. Noh, H.; Kung, C.-W.; Otake, K.-I.; Peters, A.W.; Li, Z.; Liao, Y.; Gong, X.; Farha, O.K.; Hupp, J.T. Redox-mediator-assisted electrocatalytic hydrogen evolution from water by a molybdenum sulfide-functionalized metal–organic framework. *ACS Catal.* **2018**, *8*, 9848–9858. [[CrossRef](#)]
66. Kung, C.-W.; Audu, C.O.; Peters, A.W.; Noh, H.; Farha, O.K.; Hupp, J.T. Copper nanoparticles installed in metal–organic framework thin films are electrocatalytically competent for CO₂ reduction. *ACS Energy Lett.* **2017**, *2*, 2394–2401. [[CrossRef](#)]
67. Nguyen, H.G.T.; Schweitzer, N.M.; Chang, C.-Y.; Drake, T.L.; So, M.C.; Stair, P.C.; Farha, O.K.; Hupp, J.T.; Nguyen, S.T. Vanadium-Node-Functionalized UiO-66: A thermally stable MOF-supported catalyst for the gas-phase oxidative dehydrogenation of cyclohexene. *ACS Catal.* **2014**, *4*, 2496–2500. [[CrossRef](#)]

68. Yang, D.; Odoh, S.O.; Wang, T.C.; Farha, O.K.; Hupp, J.T.; Cramer, C.J.; Gagliardi, L.; Gates, B.C. Metal–organic framework nodes as nearly ideal supports for molecular catalysts: NU-1000- and UiO-66-supported iridium complexes. *J. Am. Chem. Soc.* **2015**, *137*, 7391–7396. [[CrossRef](#)]
69. Pi, Y.; Feng, X.; Song, Y.; Xu, Z.; Li, Z.; Lin, W.B. Metal–organic frameworks integrate cu photosensitizers and secondary building unit-supported fe catalysts for photocatalytic hydrogen evolution. *J. Am. Chem. Soc.* **2020**, *142*, 10302–10307. [[CrossRef](#)]
70. An, B.; Li, Z.; Song, Y.; Zhang, J.; Zeng, L.; Wang, C.; Lin, W. Cooperative copper centres in a metal–organic framework for selective conversion of CO₂ to ethanol. *Nat. Chem.* **2019**, *2*, 709–717. [[CrossRef](#)]
71. Ji, P.; Manna, K.; Lin, Z.; Feng, X.; Urban, A.; Song, Y.; Lin, W. Single-Site Cobalt Catalysts at New Zr₁₂(μ₃-O)₈(μ₃-OH)₈(μ₂-OH)₆ metal–organic framework nodes for highly active hydrogenation of nitroarenes, nitriles, and isocyanides. *J. Am. Chem. Soc.* **2017**, *139*, 7004–7011. [[CrossRef](#)] [[PubMed](#)]
72. Ji, P.; Song, Y.; Drake, T.; Veroneau, S.S.; Lin, Z.; Pan, X.; Lin, W. Titanium(III)-oxo clusters in a metal–organic framework support single-site Co(II)-hydride catalysts for arene hydrogenation. *J. Am. Chem. Soc.* **2018**, *140*, 433–440. [[CrossRef](#)]
73. Comito, R.J.; Fritzsche, K.J.; Sundell, B.J.; Schmidt-Rohr, K.; Dincă, M. Single-site heterogeneous catalysts for olefin polymerization enabled by cation exchange in a metal–organic framework. *J. Am. Chem. Soc.* **2016**, *138*, 10232–10237. [[CrossRef](#)]
74. Lollar, C.T.; Qin, J.-S.; Pang, J.; Yuan, S.; Becker, B.; Zhou, H.-C. Interior decoration of stable metal–organic frameworks. *Langmuir* **2018**, *34*, 13795–13807. [[CrossRef](#)] [[PubMed](#)]
75. Brozek, C.K.; Bellarosa, L.; Soejima, T.; Clark, T.V.; López, N.; Dincă, M. Solvent-dependent cation exchange in metal–organic frameworks. *Chem. Eur. J.* **2014**, *20*, 6871–6874. [[CrossRef](#)]
76. Kim, M.; Cahill, J.F.; Fei, H.; Prather, K.A.; Cohen, S.M. Postsynthetic ligand and cation exchange in robust metal–organic frameworks. *J. Am. Chem. Soc.* **2012**, *134*, 18082–18088. [[CrossRef](#)] [[PubMed](#)]
77. Das, S.; Kim, H.; Kim, K. Metathesis in single crystal: Complete and reversible exchange of metal ions constituting the frameworks of metal–organic frameworks. *J. Am. Chem. Soc.* **2009**, *131*, 3814–3815. [[CrossRef](#)] [[PubMed](#)]
78. Denysenko, D.; Werner, T.; Grzywa, M.; Puls, A.; Hagen, V.; Eicklerling, G.; Jelic, J.; Reuter, K.; Volkmer, D. Reversible gas-phase redox processes catalyzed by Co-exchanged MFU-4l(arge). *Chem. Commun.* **2012**, *48*, 1236–1238. [[CrossRef](#)]
79. Sun, D.; Sun, F.; Deng, X.; Li, Z. Mixed-Metal Strategy on Metal–organic frameworks (MOFs) for functionalities expansion: Co substitution induces aerobic oxidation of cyclohexene over inactive Ni-MOF-74. *Inorg. Chem.* **2015**, *54*, 8639–8643. [[CrossRef](#)]
80. Zou, L.; Feng, D.; Liu, T.-F.; Chen, Y.-P.; Yuan, S.; Wang, K.; Wang, X.; Fordham, S.; Zhou, H.-C. A versatile synthetic route for the preparation of titanium metal–organic frameworks. *Chem. Sci.* **2016**, *7*, 1063–1069. [[CrossRef](#)]
81. Huxley, M.; Coghlan, C.J.; Burgun, A.; Tarzia, A.; Sumida, K.; Sumby, C.J.; Doonan, C.J. Site-specific metal and ligand substitutions in a microporous Mn²⁺-based metal–organic framework. *Dalton Trans.* **2016**, *45*, 4431–4438. [[CrossRef](#)]
82. Banerjee, P.C.; Lobo, D.E.; Middag, R.; Ng, W.K.; Shaibani, M.E.; Majumder, M. Electrochemical capacitance of Ni-doped metal organic framework and reduced graphene oxide composites: More than the sum of its parts. *ACS Appl. Mater. Interfaces* **2015**, *7*, 3655–3664. [[CrossRef](#)] [[PubMed](#)]
83. Xiao, D.J.; Bloch, E.D.; Mason, J.A.; Queen, W.L.; Hudson, M.R.; Planas, N.; Borycz, J.; Dzubak, A.L.; Verma, P.; Lee, K.; et al. Oxidation of ethane to ethanol by N₂O in a metal–organic framework with coordinatively unsaturated iron(II) sites. *Nat. Chem.* **2014**, *6*, 590. [[CrossRef](#)]
84. Li, H.; Shi, W.; Zhao, K.; Li, H.; Bing, Y.; Cheng, P. Enhanced hydrostability in Ni-doped MOF-5. *Inorg. Chem.* **2012**, *51*, 9200–9207. [[CrossRef](#)]
85. Botas, J.A.; Calleja, G.; Sánchez-Sánchez, M.; Orcajo, M.G. Cobalt doping of the MOF-5 framework and its effect on gas-adsorption properties. *Langmuir* **2010**, *26*, 5300–5303. [[CrossRef](#)] [[PubMed](#)]
86. Liu, L.; Telfer, S.G. Systematic ligand modulation enhances the moisture stability and gas sorption characteristics of quaternary metal–organic frameworks. *J. Am. Chem. Soc.* **2015**, *137*, 3901–3909. [[CrossRef](#)] [[PubMed](#)]
87. Kaye, S.S.; Dailly, A.; Yaghi, O.M.; Long, J.R. Impact of preparation and handling on the hydrogen storage properties of Zn₄O(1,4-benzenedicarboxylate)₃ (MOF-5). *J. Am. Chem. Soc.* **2007**, *129*, 14176–14177. [[CrossRef](#)] [[PubMed](#)]
88. Cychosz, K.A.; Matzger, A.J. Water stability of microporous coordination polymers and the adsorption of pharmaceuticals from water. *Langmuir* **2010**, *26*, 17198–17202. [[CrossRef](#)]
89. Drake, T.; Ji, P.; Lin, W. Site isolation in metal–organic frameworks enables novel transition metal catalysis. *Acc. Chem. Res.* **2018**, *51*, 2129–2138. [[CrossRef](#)]
90. Pascanu, V.; Miera, G.G.; Inge, A.K.; Martin-Matute, B. Metal–organic frameworks as catalysts for organic synthesis: A critical perspective. *J. Am. Chem. Soc.* **2019**, *141*, 7223–7234. [[CrossRef](#)]
91. Paciello, R.A. High Throughput screening of homogeneous catalysts: Selected trends and applications in process development. In *Applied Homogeneous Catalysis with Organometallic Compounds*, 3rd ed.; Wiley-VCH Verlag GmbH & Co. KGaA: Weinheim, Germany, 2019; pp. 1085–1096.
92. Schaub, T.; Paciello, R.A.; Limbach, M. Homogeneous catalysis with CO₂ as a building block: An industrial perspective. In *Applied Homogeneous Catalysis with Organometallic Compounds*, 3rd ed.; Wiley-VCH Verlag GmbH & Co. KGaA: Weinheim, Germany, 2019; pp. 1601–1614.
93. Manna, K.; Ji, P.; Greene, F.X.; Lin, W. Metal–organic framework nodes support single-site magnesium-alkyl catalysts for hydroboration and hydroamination reactions. *J. Am. Chem. Soc.* **2016**, *138*, 7488–7491. [[CrossRef](#)]

94. Yang, X.; Yuan, S.; Zou, L.; Drake, H.; Zhang, Y.; Qin, J.; Alsalme, A.; Zhou, H.-C. One-step synthesis of hybrid core-shell metal-organic frameworks. *Angew. Chem. Int. Ed.* **2018**, *57*, 3927–3932. [[CrossRef](#)] [[PubMed](#)]
95. Thiam, Z.; Abou-Hamad, E.; Dereli, B.; Liu, L.; Emwas, A.-H.; Ahmad, R.; Jiang, H.; Isah, A.A.; Ndiaye, P.B.; Taoufik, M.; et al. Extension of surface organometallic chemistry to metal-organic frameworks: Development of a well-defined single site [(\equiv Zr-O-)W(=O)(CH₂tBu)₃] olefin metathesis catalyst. *J. Am. Chem. Soc.* **2020**, *142*, 16690–16703. [[CrossRef](#)]
96. Yuan, S.; Zou, L.; Qin, J.-S.; Li, J.; Huang, L.; Feng, L.; Wang, X.; Bosch, M.; Alsalme, A.; Cagin, T.; et al. Construction of hierarchically porous metal-organic frameworks through linker labilization. *Nat. Commun.* **2017**, *8*, 15356. [[CrossRef](#)] [[PubMed](#)]
97. Molnar, A. (Ed.) *Palladium-Catalyzed Coupling Reactions: Practical Aspects and Future Developments*; Wiley-VCH Verlag GmbH & Co. KGaA: Weinheim, Germany, 2013; p. 570. [[CrossRef](#)]
98. De Vries, A.H.M.; Parlevliet, F.J.; Schmieder-Van De Vondervoort, L.; Mommers, J.H.M.; Henderickx, H.J.W.; Walet, M.A.M.; De Vries, J.G. A practical recycle of a ligand-free palladium catalyst for Heck reactions. *Adv. Synth. Catal.* **2002**, *344*, 996–1002. [[CrossRef](#)]
99. Wei, Y.-L.; Li, Y.; Chen, Y.-Q.; Dong, Y.; Yao, J.-J.; Han, X.-Y.; Dong, Y.-B. Pd(II)-NHDC-functionalized UiO-67 type MOF for catalyzing Heck cross-coupling and intermolecular benzyne-benzyne-alkene insertion reactions. *Inorg. Chem.* **2018**, *57*, 4379–4386. [[CrossRef](#)]
100. Bahadori, M.; Tangestaninejad, S.; Moghadam, M.; Mirkhani, V.; Mechler, A.; Mohammadpoor-Baltork, I.; Zadehahmadi, F. Metal organic framework-supported N-heterocyclic carbene palladium complex: A highly efficient and reusable heterogeneous catalyst for Suzuki-Miyaura C-C coupling reaction. *Microporous Mesoporous Mater.* **2017**, *253*, 102–111. [[CrossRef](#)]
101. Chen, L.; Rangan, S.; Li, J.; Jiang, H.; Li, Y. A molecular Pd(II) complex incorporated into a MOF as a highly active single-site heterogeneous catalyst for C-Cl bond activation. *Green Chem.* **2014**, *16*, 3978–3985. [[CrossRef](#)]
102. Fei, H.; Cohen, S.M. A robust, catalytic metal-organic framework with open 2,2'-bipyridine sites. *Chem. Commun.* **2014**, *50*, 4810–4812. [[CrossRef](#)]
103. Chen, Y.-Z.; Jiang, H.-L. Porphyrinic metal-organic framework catalyzed Heck-reaction: Fluorescence “turn-on” sensing of Cu(II) ion. *Chem. Mater.* **2016**, *28*, 6698–6704. [[CrossRef](#)]
104. Godula, K.; Sames, D. C-H bond functionalization in complex organic synthesis. *Science* **2006**, *312*, 67–72. [[CrossRef](#)]
105. Schwach, P.; Pan, X.; Bao, X. Direct conversion of methane to value-added chemicals over heterogeneous catalysts: Challenges and prospects. *Chem. Rev.* **2017**, *117*, 8497–8520. [[CrossRef](#)]
106. Liao, P.; Getman, R.B.; Snurr, R.Q. Optimizing open iron sites in metal-organic frameworks for ethane oxidation: A first-principles study. *ACS Appl. Mater. Interfaces* **2017**, *9*, 33484–33492. [[CrossRef](#)]
107. Bergman, R.G. Organometallic chemistry: C-H activation. *Nature* **2007**, *446*, 391–393. [[CrossRef](#)] [[PubMed](#)]
108. Santoro, S.; Kozhushkov, S.I.; Ackermann, L.; Vaccaro, L. Heterogeneous catalytic approaches in C-H activation reactions. *Green Chem.* **2016**, *18*, 3471–3493. [[CrossRef](#)]
109. Qin, J.-S.; Yuan, S.; Lollar, C.; Pang, J.; Alsalme, A.; Zhou, H.-C. Stable metal-organic frameworks as a host platform for catalysis and biomimetics. *Chem. Commun.* **2018**, *54*, 4231–4249. [[CrossRef](#)]
110. Sawano, T.; Lin, Z.; Boures, D.; An, B.; Wang, C.; Lin, W. Metal-organic frameworks stabilize mono(phosphine)-metal complexes for broad-scope catalytic reactions. *J. Am. Chem. Soc.* **2016**, *138*, 9783–9786. [[CrossRef](#)]
111. Zhang, Y.; Li, J.; Yang, X.; Zhang, P.; Pang, J.; Li, B.; Zhou, H.-C. A mesoporous NNN-pincer-based metal-organic framework scaffold for the preparation of noble-metal-free catalysts. *Chem. Commun.* **2019**, *55*, 2023–2026. [[CrossRef](#)] [[PubMed](#)]
112. Kalaj, M.; Cohen, S.M. Postsynthetic modification: An enabling technology for the advancement of metal-organic frameworks. *ACS Cent. Sci.* **2020**, *6*, 1046–1057. [[CrossRef](#)]
113. Anderson, J.S.; Gallagher, A.T.; Mason, J.A.; Harris, T.D. A five-coordinate heme dioxygen adduct isolated within a metal-organic framework. *J. Am. Chem. Soc.* **2014**, *136*, 16489–16492. [[CrossRef](#)] [[PubMed](#)]
114. Gallagher, A.T.; Lee, J.Y.; Kathiresan, V.; Anderson, J.S.; Hoffman, B.M.; Harris, T.D. A structurally-characterized peroxomanganese(IV) porphyrin from reversible O₂ binding within a metal-organic framework. *Chem. Sci.* **2018**, *9*, 1596–1603. [[CrossRef](#)] [[PubMed](#)]
115. Brozek, C.K.; Miller, J.T.; Stoian, S.A.; Dincă, M. NO disproportionation at a mononuclear site-isolated Fe²⁺ center in Fe²⁺-MOF-5. *J. Am. Chem. Soc.* **2015**, *137*, 7495–7501. [[CrossRef](#)]
116. Bloch, E.D.; Queen, W.L.; Chavan, S.; Wheatley, P.S.; Zdrozny, J.M.; Morris, R.; Brown, C.M.; Lamberti, C.; Bordiga, S.; Long, J.R. Gradual release of strongly bound nitric oxide from Fe₂(NO)₂(dobdc). *J. Am. Chem. Soc.* **2015**, *137*, 3466–3469. [[CrossRef](#)]
117. Rieth, A.J.; Tulchinsky, Y.; Dinca, M. High and reversible ammonia uptake in mesoporous azolate metal organic frameworks with open Mn, Co, and Ni sites. *J. Am. Chem. Soc.* **2016**, *138*, 9401–9404. [[CrossRef](#)]
118. Reed, D.A.; Keitz, B.K.; Oktawiec, J.; Mason, J.A.; Runcevski, T.; Xiao, D.J.; Darago, L.E.; Crocella, V.; Bordiga, S.; Long, J.R. A spin transition mechanism for cooperative adsorption in metal-organic frameworks. *Nature* **2017**, *550*, 96–100. [[CrossRef](#)]
119. Reed, D.A.; Xiao, D.J.; Gonzalez, M.I.; Darago, L.E.; Herm, Z.R.; Grandjean, F.; Long, J.R. Reversible CO scavenging via adsorbate-dependent spin state transitions in an iron(II)-triazolate metal-organic framework. *J. Am. Chem. Soc.* **2016**, *138*, 5594–5602. [[CrossRef](#)]
120. Bloch, E.D.; Queen, W.L.; Krishna, R.; Zdrozny, J.M.; Brown, C.M.; Long, J.R. Hydrocarbon separations in a metal-organic framework with open iron(II) coordination sites. *Science* **2012**, *335*, 1606. [[CrossRef](#)]

121. Tulchinsky, Y.; Hendon, C.H.; Lomachenko, K.A.; Borfecchia, E.; Melot, B.C.; Hudson, M.R.; Tarver, J.D.; Korzynski, M.D.; Stubbs, A.W.; Kagan, J.J.; et al. Reversible capture and release of Cl₂ and Br₂ with a redox-active metal-organic framework. *J. Am. Chem. Soc.* **2017**, *139*, 5992–5997. [[CrossRef](#)] [[PubMed](#)]
122. Zeng, M.H.; Yin, Z.; Tan, Y.X.; Zhang, W.X.; He, Y.P.; Kurmoo, M. Nanoporous cobalt(II) MOF exhibiting four magnetic ground states and changes in gas sorption upon post-synthetic modification. *J. Am. Chem. Soc.* **2014**, *136*, 4680–4688. [[CrossRef](#)] [[PubMed](#)]
123. Motokawa, N.; Miyasaka, H.; Yamashita, M.; Dunbar, K.R. An electron-transfer ferromagnet with T_c=107 K based on a three-dimensional [Ru-2](2)/TCNQ system. *Angew. Chem. Int. Ed.* **2008**, *47*, 7760–7763. [[CrossRef](#)]
124. Stone, K.H.; Stephens, P.W.; McConnell, A.C.; Shurdha, E.; Pokhodnya, K.I.; Miller, J.S. Mn-II(TCNE)(3/2)(I-3)(1/2)-A 3D network-structured organic-based magnet and comparison to a 2D analog. *Adv. Mater.* **2010**, *22*, 2514–2519. [[CrossRef](#)]
125. Lapidus, S.H.; McConnell, A.C.; Stephens, P.W.; Miller, J.S. Structure and magnetic ordering of a 2-D Mn-II (TCNE)I(OH₂) (TCNE = tetracyanoethylene) organic-based magnet (T_c = 171 K). *Chem. Commun.* **2011**, *47*, 7602–7604. [[CrossRef](#)] [[PubMed](#)]
126. Jeon, I.R.; Negru, B.; Van Duyne, R.P.; Harris, T.D. A 2D Semiquinone Radical-Containing Microporous Magnet with Solvent-Induced Switching from T_c=26 to 80 K. *J. Am. Chem. Soc.* **2015**, *137*, 15699–15702. [[CrossRef](#)]
127. DeGayner, J.A.; Jeon, I.R.; Sun, L.; Dinca, M.; Harris, T.D. 2D Conductive Iron-Quinoid Magnets Ordering up to T_c=105 K via Heterogenous Redox Chemistry. *J. Am. Chem. Soc.* **2017**, *139*, 4175–4184. [[CrossRef](#)]
128. Zadrozny, J.M.; Gallagher, A.T.; Harris, T.D.; Freedman, D.E. A Porous Array of Clock Qubits. *J. Am. Chem. Soc.* **2017**, *139*, 7089–7094. [[CrossRef](#)] [[PubMed](#)]
129. Yu, C.-J.; Krzyaniak, M.D.; Fataftah, M.S.; Wasielewski, M.R.; Freedman, D.E. A concentrated array of copper porphyrin candidate qubits. *Chem. Sci.* **2019**. [[CrossRef](#)] [[PubMed](#)]
130. Taylor-Pashow, K.M.L.; Della Rocca, J.; Xie, Z.G.; Tran, S.; Lin, W.B. Postsynthetic modifications of iron-carboxylate nanoscale metal-organic frameworks for imaging and drug delivery. *J. Am. Chem. Soc.* **2009**, *131*, 14261–14263. [[CrossRef](#)] [[PubMed](#)]
131. He, C.; Lu, K.; Liu, D.; Lin, W. Nanoscale metal-organic frameworks for the Co-delivery of cisplatin and pooled siRNAs to enhance therapeutic efficacy in drug-resistant ovarian cancer cells. *J. Am. Chem. Soc.* **2014**, *136*, 5181–5184. [[CrossRef](#)]
132. Ni, K.Y.; Lan, G.X.; Veroneau, S.S.; Duan, X.P.; Song, Y.; Lin, W.B. Nanoscale metal-organic frameworks for mitochondria-targeted radiotherapy-radiodynamic therapy. *Nat. Commun.* **2018**, *9*, 4321. [[CrossRef](#)]
133. Lan, G.X.; Ni, K.Y.; Veroneau, S.S.; Song, Y.; Lin, W.B. Nanoscale metal-organic layers for radiotherapy-radiodynamic therapy. *J. Am. Chem. Soc.* **2018**, *140*, 16971–16975. [[CrossRef](#)] [[PubMed](#)]
134. Diring, S.; Carne-Sanchez, A.; Zhang, J.C.; Ikemura, S.; Kim, C.; Inaba, H.; Kitagawa, S.; Furukawa, S. Light responsive metal-organic frameworks as controllable CO-releasing cell culture substrates. *Chem. Sci.* **2017**, *8*, 2381–2386. [[CrossRef](#)] [[PubMed](#)]